Universidade do Minho
Escola de Medicina

Maria Inês Antunes Pereira

Studying the impact of hyperglycemia in chick lung branching morphogenesis

outubro de 2022

Studying the impact of hyperglycemia in chick lung branching morphogenesis

Inês Pereira

UMinho | 2022

Universidade do Minho
Escola de Medicina

Maria Inês Antunes Pereira

Studying the impact of hyperglycemia in chick lung branching morphogenesis

Dissertação de Mestrado
Ciências da Saúde

Trabalho efetuado sob a orientação de
Doutora Rute Carina Silva Moura
Professor Doutor Jorge Manuel Nunes Correia Pinto

outubro de 2022

Acknowledgements

This thesis is the result of two years of work to which many people contributed, and which made me grow not only as a scientist but also as a person, and I am very grateful for that.

First of all, I would like to thank my supervisors, Rute Moura and Prof Jorge Correia Pinto, for the opportunity to work on their research project. To Rute, thank you for your availability to teach me everything, from the most basic things to the hardest ones. Thank you for being patient with me, for all the time you dedicated to me and most of all, for all the motivation when things were not going so well in the lab. Thank you!

To all my lab colleagues, especially Inês, Daniela, and Hugo, thank you for all the help and the advice that you taught me in the lab and helped me in the trickiest situations. Thank you for all the lunches together and also the group dinners! To my master colleagues, thank you for the support and for being all together during these years through all situations.

To Filipa, thank you for your friendship and support during these years and for being with me since day 1 of university, it's been almost 6 years! Even far away from each other, it is amazing to know that our relationship remains the same, with our "monthly podcasts". Miss you!

To my friends in Barcelos, thank you for being patient with me, for all the motivation and friendship. To Marisa and Xavi, thanks for the dinners, sangrias, travels and all the funny moments together!

Thank you to Diogo, the one that is with me every day in every moment, good and worst ones. Thank you for your patience, motivation, advice, and most importantly, for your love. These last two years have been an adventure and thanks for always being with me no matter what. Love you!

To my sister Ana, thank you for everything, all the help, opinions, motivation, and inspiration. Thanks Ana and Diogo2, for the dinners, video calls and all the beers and sunsets in Porto. Love you!

Lastly, to my parents, thank you for all your support throughout all these years, thank you for making me the person I am today. Thank you!

Financial Support

This work has been funded by National funds, through the Foundation for Science and Technology (FCT) – project UIDB/50026/2020 and UIDP/50026/2020.

FCT
Fundação para a Ciência e a Tecnologia

STATEMENT OF INTEGRITY

I hereby declare having conducted this academic work with integrity. I confirm that I have not used plagiarism or any form of undue use of information or falsification of results along the process leading to its elaboration.

I further declare that I have fully acknowledged the Code of Ethical Conduct of the University of Minho.

RESUMO

O Estudo do impacto da hiperglicemia no desenvolvimento pulmonar da galinha

A hiperglicemia na gravidez é considerada um problema de saúde pública, estimando-se que aproximadamente uma em seis gravidezes são afetadas. No primeiro trimestre da gravidez, a hiperglicemia não controlada pode afetar a organogénese, resultando em malformações congénitas severas. Anomalias nos sistemas craniofacial, cardiovascular, gastrointestinal, urogenital, musculoesquelético e nervoso central têm sido associadas com a diabetes na gravidez. No entanto, o impacto da hiperglicemia no desenvolvimento do pulmão ainda não foi explorado.

Assim, o principal objetivo deste projeto é estudar o impacto da hiperglicemia no processo de ramificação pulmonar, usando explantes de pulmão do embrião de galinha *in vitro*, expostos a diferentes concentrações de glucose. Após a cultura de explantes de pulmão, foi realizada uma análise morfométrica e de ramificação do pulmão, e os explantes foram também processados para estudos de expressão de genes. Desta forma, o padrão de expressão dos recetores de insulina e IGF (*igr1r*, *igf2r*, *insr*), das enzimas lactato desidrogenase (*ldha*, *ldhb*) e genes relacionados com a diferenciação do tecido pulmonar (*sox2* e *sox9*), foram avaliados por hibridização *in situ.* Além disso, os níveis de expressão de transportadores de glucose (*glut1*, *glut3*), enzimas do catabolismo da glucose (*hk1*, *pfk1*) e genes relacionados com o processo de ramificação do pulmão (*fgf10*, *shh* e *wnt7b*), foram avaliados por qPCR.

Os explantes de pulmão expostos a níveis elevados de glucose apresentaram uma diminuição da área total do pulmão, e da área e perímetro epitelial do pulmão, assim como uma diminuição no número de brônquios secundários formados após a cultura de explantes. Além do mais, os transportadores de glucose e as enzimas glicolíticas também estavam diminuídos, exceto a enzima *ldhb*, que aumentou a sua expressão nos pulmões expostos a níveis elevados de glucose. Os níveis de expressão de *fgf10*, *shh* e *wnt7b,* importantes para a ramificação do pulmão em desenvolvimento, também se mostraram alterados como consequência da exposição da hiperglicemia. Assim, estas alterações moleculares podem explicar o impacto morfológico observado no pulmão embrionário de galinha, como consequência de hiperglicemia. Em suma, estes resultados mostram que a hiperglicemia pode ter impacto na organogénese do pulmão de galinha ao nível morfológico, metabólico e molecular. Este trabalho contribui para averiguar os potenciais efeitos adversos da hiperglicemia na organogénese do pulmão, que podem contribuir para o desenvolvimento de malformações congénitas e outras complicações respiratórias.

Palavras-chave: Hiperglicemia na gravidez, desenvolvimento pulmonar, ramificação pulmonar, embrião de galinha

ABSTRACT

Studying the impact of hyperglycemia in chick lung branching morphogenesis

Hyperglycemia in pregnancy is considered a major public health concern, and it is estimated that it can affect approximately one in six pregnancies. Uncontrolled hyperglycemia in the first trimester of pregnancy can affect organogenesis, resulting in severe congenital malformations. Abnormalities in craniofacial, cardiovascular, gastrointestinal, urogenital, musculoskeletal, and central nervous systems have been associated with diabetes in pregnancy. However, the impact of hyperglycemia on early lung development has not been explored yet.

In this sense, the main goal of this project is to study the impact of hyperglycemia in early lung branching morphogenesis using *in vitro* chick lung explants exposed to different glucose concentrations. After lung explant culture, branching and morphometric analysis were performed, and lung explants were also processed for gene expression studies. The expression pattern of insulin/IGF receptors (*igr1r*, *igf2r*, *insr*), lactate dehydrogenase enzymes (*ldha*, *ldhb*), and lung patterning-related genes (*sox2* and *sox9*) were assessed by *in situ* hybridization. Furthermore, expression levels for glucose transporters (*glut1*, *glut3*), glucose catabolism enzymes (*hk1*, *pfk1*), and lung branching-related genes (*fgf10*, *shh* and *wnt7b*) were evaluated by qPCR.

Lung explants treated with high glucose levels exhibited a decrease in the total area, the epithelial area and perimeter of the lung, and a reduced number of secondary buds formed after 48-hour culture. Moreover, glucose transporters and glycolytic enzymes expression levels were also decreased, except for *ldhb*, which showed increased expression in glucose-treated embryonic lungs. Regarding the expression levels of *fgf10*, *shh* and *wnt7b*, important players underlying lung branching morphogenesis, an impairment was also observed as a consequence of hyperglycemia exposure. Overall, these molecular alterations might explain the hyperglycemic-related morphological impact observed in the chick embryonic lung. Altogether, these results imply that hyperglycemia exposure can impair early chick lung organogenesis at the morphological, metabolic, and molecular levels. This work brings new insights into the potential adverse effects of hyperglycemia on early lung organogenesis that may ultimately contribute to developing congenital lung malformations and other abnormal respiratory outcomes.

Keywords: Hyperglycemia in pregnancy, lung development, branching morphogenesis, chicken embryo

Table of Contents

Acknowledgements iii

Resumo v

Abstract vi

List of Abbreviations ix

List of Figures x

List of Tables xii

1. Introduction 1

1.1 Diabetes *mellitus* 1

1.2 Hyperglycemia in pregnancy 2

1.3 Embryonic Development 4

1.4 Chicken embryo model 5

1.5 Chick lung development 6

1.5.1 Respiratory progenitors 6

1.5.2 Branching morphogenesis 8

1.6 Metabolism and embryonic development 10

2. Aims 13

3. Material and Methods 14

3.1. Ethical Statement 14

3.2. Tissue Collection 14

3.3. *In vitro* lung explant culture 14

3.4. Morphometric and Branching analysis 15

3.5. Whole mount *in situ* hybridization 15

3.5.1. RNA probe synthesis 15

3.5.1.1. Cloning protocol 15

3.5.1.2. *In vitro* transcription 17
3.5.2. *In situ* hybridization protocol 18
3.6. Histological Sections 19
3.7. Quantitative real-time PCR (qPCR) 19
3.8. Statistical analysis 20
4. Results 21
4.1. Impact of hyperglycemia on lung branching and growth 21
4.2. Impact of hyperglycemia on insulin-related gene expression 23
4.2.1. Characterization of the expression pattern of insulin and IGF receptors 24
4.2.2. Impact of high glucose levels in the expression of insulin and IGF receptors 26
4.3. Impact of hyperglycemia in key metabolic players 27
4.4. Lung patterning and branching-related gene expression in hyperglycemia exposed lungs 29
5. Discussion 31
6. Final Remarks and Future Perspectives 37
7. References 39
8. Appendix I 46

List of Abbreviations

BMP4 – Bone morphogenetic protein 4

DIP – Diabetes in pregnancy

DM – Diabetes *mellitus*

DTT – Dithiothreitol

EDTA – Ethylenediaminetetraacetic acid

EGF – Epidermal growth factor

EGTA – Egtazic acid

FGF – Fibroblast growth factor

FGF2R – Fibroblast growth factor 2 receptor

FZD – Frizzled

GDM – Gestational diabetes *mellitus*

GLUT – Glucose transporter

HbA1c – Hemoglobin A1c

HH – Hamburger-Hamilton

HHIP – Hedgehog-interacting protein

HK1 – Hexokinase 1

ICM – Inner cell mass

IFG – Impaired fasting glucose

IGF – Insulin growth factor

IGFR – Insulin growth factor receptor

IGT – Impaired glucose tolerance

INSR – Insulin receptor

LDH – Lactate dehydrogenase

MABT – Maleic acid buffer with Tween 20

OGTT – Oral glucose tolerance test

OXPHOS – Oxidative Phosphorylation

PBS – Phosphate-buffered saline

PBT - Phosphate-buffered saline with Tween 20

PDH – Pyruvate dehydrogenase

PEP – Phosphoenolpyruvate

PFK1 – Phosphofructokinase 1

PKM2 – Pyruvate kinase M2

PSM – Presomitic mesoderm

PTCH – Patched

qPCR - Quantitative polymerase chain reaction

RNasin – Ribonuclease inhibitor

SHH – Sonic Hedgehog

SMO – Smoothened

SOX2/9 – SRY-Box Transcription Factor 2/9

SPRY2 – Sprouty 2

T1DM – Type 1 diabetes *mellitus*

T2DM – Type 2 diabetes *mellitus*

TBX4 – T-box transcription factor 4

WHO – World Health Organization

WNT – Wingless-related Integrated Site

List of Figures

Figure 1 - Hyperglycemia in pregnancy and respiratory outcomes for the offspring, considering the timing of hyperglycemia exposure. 4

Figure 2 – Schematic representation of chick embryonic respiratory tract development. 7

Figure 3 - Overview of molecular signaling pathways during lung branching morphogenesis and its epithelial-mesenchymal interactions. 10

Figure 4 – Representation of the different functions of metabolism and its respective roles. 11

Figure 5 - *In vitro* chick lung explant culture exposed to different glucose concentrations. 21

Figure 6 - Morphometric and branching analysis of chick lung explants exposed to 5.5 mM (control), 25 mM, 50 mM or 75 mM of glucose 23

Figure 7 - Characterization of *igf1r* expression pattern during embryonic chick lung development. 24

Figure 8 - Characterization of *igf2r* expression pattern during embryonic chick lung development. ... 25

Figure 9 - Characterization of *insr* expression pattern during embryonic chick lung development. 25

Figure 10 - *In vitro* chick lung explants supplemented with glucose, followed by *in situ* hybridization for *igf1r*, *igf2r* and *insr*. 26

Figure 11 - mRNA expression levels of glucose transporters (*glut1* and *glut3*) and glucose catabolism related enzymes (*hk1* and *pfk1*) evaluated by qPCR. 27

Figure 12 - *In vitro* chick lung explants supplemented with glucose, followed by *in situ* hybridization for *ldha* and *ldhb*. 28

Figure 13 - *In vitro* chick lung explants supplemented with glucose, followed by *in situ* hybridization for *sox2* and *sox9*. 29

Figure 14 - mRNA expression levels of branching-related genes evaluated by qPCR 30

Figure 15 – Representation of the impact of hyperglycemia in glucose metabolism of the chick embryonic lung 34

Supplementary Figure 1 – Primer testing for *igf1r*, *igf2r* and *insr*.....46

Supplementary Figure 2 – *igf1r*, *igf2r* and *insr* expression pattern in the chicken embryo..... 46

List of Tables

Table 1 - Primer sequences forward (Fw) and reverse (Rv) used for *in situ* hybridization and its annealing temperature and fragment expected size. 17

Table 2 - RNA polymerase and the corresponding supplier and transcription buffer used for *in vitro* transcription during RNA probe synthesis for each gene. 18

Table 3 - Primer sequences forward (Fw) and reverse (Rv) used for qPCR and its annealing temperatures and fragment expected size. 20

1. Introduction

1.1 Diabetes *mellitus*

Diabetes *mellitus* (DM) is a chronic metabolic disease that is steadily increasing in prevalence over the last decades, being considered by the World Health Organization (WHO) as a major public health concern (WHO, 2016). It is estimated that approximately 537 million people worldwide suffer from DM, and it is projected that this number will increase by approximately 50% in 2045 (Sun *et al.*, 2022). DM can be responsible for several complications, such as chronic kidney disease, cardiovascular diseases, nerve damage, retinopathy, and foot ulceration (IDF, 2021). Besides, it is known that, in 2021, around 6.7 million people will have died due to DM or its complications (IDF, 2021).

Diabetes is characterized by high blood glucose levels, namely hyperglycemia. It occurs when the body cannot produce enough insulin or due to its incapacity to use the insulin it produces. Insulin is a hormone secreted by the β cells of the pancreatic islets, and its main function is to regulate blood glucose levels, allowing glucose to enter the cells, where it will be stored and used as an energy source (Rahman *et al.*, 2021). DM is classified as type 1 diabetes mellitus (T1DM) or type 2 diabetes mellitus (T2DM). T1DM occurs due to autoimmune destruction of pancreatic β cells, resulting in decreased insulin production and, consequently, hyperglycemia (DiMeglio *et al.*, 2019). T1DM is most frequently diagnosed in children and young adults and is associated with various symptoms, such as polyuria, polydipsia, blurred vision, and weight loss, as the most common ones (Craig *et al.*, 2009). On the other hand, T2DM consists of the incapacity of the cells to respond to insulin, most of the time associated with insulin resistance, resulting in a decrease in the uptake of glucose by the muscle and adipose tissue, leading to increased blood glucose levels (Zheng *et al.*, 2018). T2DM is responsible for approximately 90% of all diabetes worldwide, and obesity has been associated as a major risk factor (IDF, 2021). The symptoms are very similar to the ones in T1DM, although patients usually have no symptoms at the first stages of the disease and remain undiagnosed until complications appear. In fact, approximately 50% of adults between 20 and 79 years old with diabetes in the world are unaware of their condition (Ogurtsova *et al.*, 2022). Thus, early diagnosis and treatment are very important at the initial stages of the disease to avoid severe complications in the future.

Diabetes is generally diagnosed by fasting plasma glucose concentration ≥7.0 mmol/L or two-hour after 75 g oral glucose tolerance test (OGTT) concentration ≥11.1 mmol/L. In the presence of symptoms, diagnosis can be based on a random venous plasma glucose concentration ≥11.1 mmol/L (Petersmann *et al.*, 2019). Hemoglobin A1c (HbA1c) can also be measured to diagnose diabetes (≥6.5%), which

determines the amount of HbA1c attached to glucose, suggesting the average level of blood glucose over the past two to three months (Petersmann *et al.*, 2019). Intermediate conditions of diabetes, usually termed "prediabetes", can also be detected when blood glucose levels are too high to be normal even though they are below the threshold to be considered diabetes. Prediabetes refers to impaired glucose tolerance (IGT) and impaired fasting glucose (IFG), resulting in a higher risk of developing T2DM and its related complications, mainly cardiovascular diseases (Punthakee *et al.*, 2018).

Patients with T1DM are typically treated with insulin injections to control blood glucose levels, while T2DM patients usually need oral medication, including antidiabetic metformin, as the most used one (Tan *et al.*, 2019). In the last case, insulin injections can also be necessary if medication alone is insufficient to control hyperglycemia or in combination with other antidiabetic drugs (Tan *et al.*, 2019). Overall, lifestyle improvement, such as a healthy diet and physical activity, is essential to prevent severe complications associated with the disease and to control blood glucose levels (IDF, 2021).

1.2 Hyperglycemia in pregnancy

Hyperglycemia is also a common complication during pregnancy, and it is estimated that it can affect approximately one in six pregnancies due to an increase in diabetic patients, including women of childbearing age (IDF, 2021). It negatively impacts both mother and child, increasing the risk of congenital malformations, stillbirth, macrosomia, and maternal morbidity and mortality (Sweeting *et al.*, 2016). Maternal diabetes is known to affect embryonic development due to the teratogenic effect of hyperglycemia. However, the severity of the consequences for the offspring will depend on the timing of the exposure, along with genetic and metabolic factors.

Hyperglycemia first detected in pregnancy can be classified as diabetes in pregnancy (DIP) or gestational diabetes *mellitus* (GDM; WHO, 2014). The first refers to women with uncontrolled and undiagnosed hyperglycemia only detected during early pregnancy, while GDM refers to temporary hyperglycemia acquired during pregnancy (Guariguata *et al.*, 2014). DIP has been associated with the worst health consequences for the offspring compared to GDM, and consequently, it has been described as a major teratogenic factor (Azad *et al.*, 2017). However, most studies do not distinguish between both types of hyperglycemia during pregnancy. In fact, diabetes is usually detected between 24 and 28 weeks of gestation, when an OGTT is recommended, by measuring plasma glucose concentration while fasting and one and two hours after 75 g glucose ingestion (Guariguata *et al.*, 2014). Thus, some pregnant women with undiagnosed diabetes onset before pregnancy can be misdiagnosed with GDM as it is usually only detected in the second trimester of pregnancy.

Uncontrolled hyperglycemia in the first trimester of pregnancy can affect organogenesis, resulting in severe congenital malformations (Ornoy *et al.*, 2021). Indeed, abnormalities in the craniofacial, cardiovascular, gastrointestinal, urogenital, musculoskeletal, and central nervous systems have been linked with DIP, resulting in impaired embryonic development (Ding *et al.*, 2020).

Conversely, GDM affects later stages of development, mostly associated with excessive fetal growth, leading to macrosomia as the most common consequence. High glucose levels in the mother will increase glucose transport across the placenta through the expression of glucose transporters (GLUTs), leading to hyperglycemia in the fetus (Ornoy *et al.*, 2021). Consequently, there is an increase in fetus adipose tissue, enhancing fetal growth (Ornoy *et al.*, 2021). Moreover, there is an increased risk of developing metabolic and cardiovascular disorders later in childhood (Bianco and Josefson, 2019).

Additionally, it is also known that the insulin/insulin-like growth factor (IGF) system impairs fetal growth and development caused by maternal hyperglycemia, due to a deregulation in the expression of IGF1, IGF2 and their receptors, insulin receptor (INSR), IGF1 receptor (IGF1R) and IGF2 receptor (IGF2R; Hiden *et al.*, 2009). However, the mechanisms behind these alterations are not well-established.

The occurrence of lung-associated defects has been related to maternal metabolic health; however, the underlying mechanisms have not been dissected so far, and there is an evident lack of information regarding hyperglycemia-related events in early lung development. Insults occurring during the early stages of embryo development increase the risk of disturbing lung organogenesis and result in congenital anomalies, whereas if development is perturbed at later stages, the impact is at the functional level (Yammine and Latzin, 2020; **Fig. 1**). In this sense, gestational diabetes delays fetal lung maturation; it disturbs surfactant protein production (Baack *et al.*, 2016), increasing the risk of respiratory distress syndrome and predisposing other respiratory diseases, such as asthma and wheezing later in childhood (Azad *et al.*, 2017). However, up to now, the impact of diabetes in pregnancy on early lung development has not been explored.

Further studies are needed to study the impact of hyperglycemia in early embryonic development, as it carries serious complications in organogenesis. Moreover, most studies focus on late stages of development and usually do not distinguish between DIP and GDM.

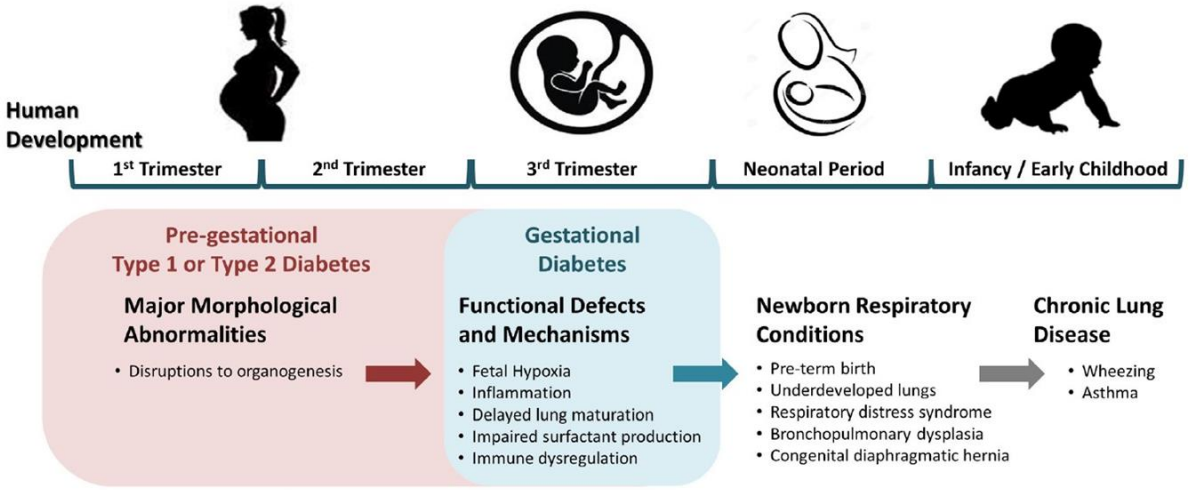

Figure 1 - Hyperglycemia in pregnancy and respiratory outcomes for the offspring, considering the timing of hyperglycemia exposure. Adapted from Azad *et. al*, 2017.

1.3 Embryonic Development

Embryonic development is characterized by the formation and organization of all organs that establish an organism. Embryonic development comprises the first eight weeks of human development, where the developing human is termed as an embryo, after which it is referred to as a fetus (Biga *et al.*, 2008).

After fertilization occurs, the zygote undergoes a series of cell divisions until the formation of a blastocyst, a spherical structure with an inner cell mass (ICM), which will later give rise to the embryo. The outer layer of the blastocyst consists of trophoblast cells, which will develop into extraembryonic tissues (el Azhar and Sonnen, 2021). The ICM will then differentiate into epiblast cells and primitive endoderm. After implantation of the blastocyst in the uterus, gastrulation occurs, meaning that epiblast cells will give rise to the three germ layers: endoderm, mesoderm, and ectoderm. Following gastrulation, organogenesis will be responsible for the formation of all organs, where cells from each germ layer will differentiate and grow into multiple tissues (Rossant and Tam, 2022). Cellular and molecular processes are highly regulated throughout organogenesis, contributing to normal organ development. Thus, insults occurring during this period can affect organogenesis, increasing the risk of congenital malformations. Moreover, this period is more sensitive to teratogens, which can impair growth and structure of the developing embryo or fetus, resulting in birth defects (Alwan and Chambers, 2015). On the other hand, if the development is perturbed at later stages of development, the impact is at the functional level

(Yammine and Latzin, 2020). Therefore, the timing of teratogenic exposure will result in different consequences.

Several animal models are used to study human developmental biology, such as the nematode *Caenorhabditis elegans*, the fruit fly *Drosophila melanogaster,* the zebrafish *Danio rerio*, the mouse *Mus Musculus* and, importantly, the chicken *Gallus gallus* (Stern, 2004). The chicken embryo model has played an essential role in understanding human development, and it has also contributed to numerous fields such as immunology, genetics, virology, cancer, and cell biology (Rashidi and Sottile, 2009).

1.4 Chicken embryo model

The first model system used in developmental studies was the chicken embryo when, around 350 BC, Aristotle first opened hen's eggs in different stages and monitored the progression of embryonic development (Wolpert, 2004). In 1951, Viktor Hamburger and Howard Hamilton described the 46 chronological stages of chicken embryo development, from laying the egg to a newly hatched chick (Hamburger and Hamilton, 1951). This illustrated series of 46 stages is known as the Hamburger-Hamilton (HH) developmental table; it is still consistently used, allowing reliable reporting regarding the staging of the chicken embryo and, consequently, the reproducibility between researchers worldwide. In the last decades, the chicken embryo has contributed to several findings regarding human embryonic development due to its several advantages over mammalian models, making it a successful animal model to study development.

The chicken embryo is an accessible, affordable, and nutritionally self-sufficient animal model. Moreover, it is easy and cheap to maintain, without the requirement of specific facilities, and it has a short incubation period of 21 days (Bjørnstad *et al.*, 2015). Importantly, the chicken embryo develops independently of the mother; thus, it is not necessary to euthanize the mother to access the embryo. Also, chicken embryo manipulation does not require *in utero* surgeries as it occurs in the mouse and rat model (Panda and McGrew, 2021). Embryo manipulation *in ovo* can be performed by cutting a small window in the eggshell, enabling access to the embryo, which can then be sealed after any manipulation performed in the chicken embryo, allowing the observation of the experiment's outcome without perturbing embryo development (Korn and Cramer, 2007). The chicken embryo can also be removed from the eggshell and cultured *ex ovo,* which may be useful for some types of embryo manipulation, for instance, in microsurgeries and imaging (Dohle *et al.*, 2010). Tissue explant *in vitro* is also described for the chicken embryo, where the organ architecture is maintained, allowing to study the impact of specific molecules in organ development (Bednarczyk *et al.*, 2021).

The main disadvantage of the chicken embryo model is the fact that it is not mammalian. Thus, translating the results obtained from the chicken embryo model to humans may sometimes be challenging. Nevertheless, the chicken is phylogenetically more similar to mammals than other animal model systems used in developmental biology, such as the zebrafish and the nematode worm (Bjørnstad *et al.*, 2015). In fact, the chicken and human genomes share approximately 70% homology; at the early stages of development, both chicken and human embryos have very similar morphology, and most of the embryonic developmental processes are also conserved (Shi *et al.*, 2014). Additionally, both are amniotes, meaning that during embryogenesis, they develop within the amnion, an extraembryonic membrane.

Due to the well-known advantages and applications of the chicken embryo model, this animal system has become widely used as a replacement for experiments with mammalian models, being a valuable tool for studying embryonic development.

1.5 Chick lung development

Lung organogenesis is a complex process consisting of epithelial-mesenchymal interactions, highly coordinated and regulated by several signaling pathways, contributing to the formation of a fully functional organ (Caldeira *et al.*, 2021). Despite the differences between mammalian and chick adult lung morphology, the molecular events underlying early lung organogenesis are very similar. For instance, the lateral branching observed in the chick lung is very similar to the domain branching that occurs during mammalian lung development (Maina, 2012); also, the signaling pathways underlying chick lung branching appear to be highly conserved between both species (Fernandes-Silva *et al.*, 2017; Moura *et al.*, 2011, 2014, 2016). Therefore, the chicken embryo model has been successfully used as an alternative to studying lung branching morphogenesis.

1.5.1 Respiratory progenitors

The primordial chick lung starts developing on day 3 of embryogenesis, emerging from the primitive foregut endoderm (Moura and Correia-Pinto, 2017). In the chicken embryo lung, the epithelial compartment derives from the endodermal germ layer, while the mesenchyme arises from the mesoderm. Moreover, the respiratory tract cell specification is characterized by the expression of the transcription factor NKX2.1 (or TTF1) in the endodermal cells of the ventral anterior foregut. Endodermal budding and splitting of the respiratory tract and esophagus is characterized by the expression of *tbx4*, a

member of conserved T-box-containing transcription factors present in the mesoderm surrounding the primordial lung (Sakiyama *et al.*, 2003). *tbx4* activates *fgf10* (fibroblast growth factor 10) expression in the mesoderm, inducing primary bud formation by triggering *nkx2.1* expression (Sakiyama *et al.*, 2003). The single lung bud will then divide into two right and left primordial buds, which will grow distally; the secondary bronchi will then emerge laterally surrounded by mesenchyme, in a process known as branching morphogenesis (**Fig. 2**).

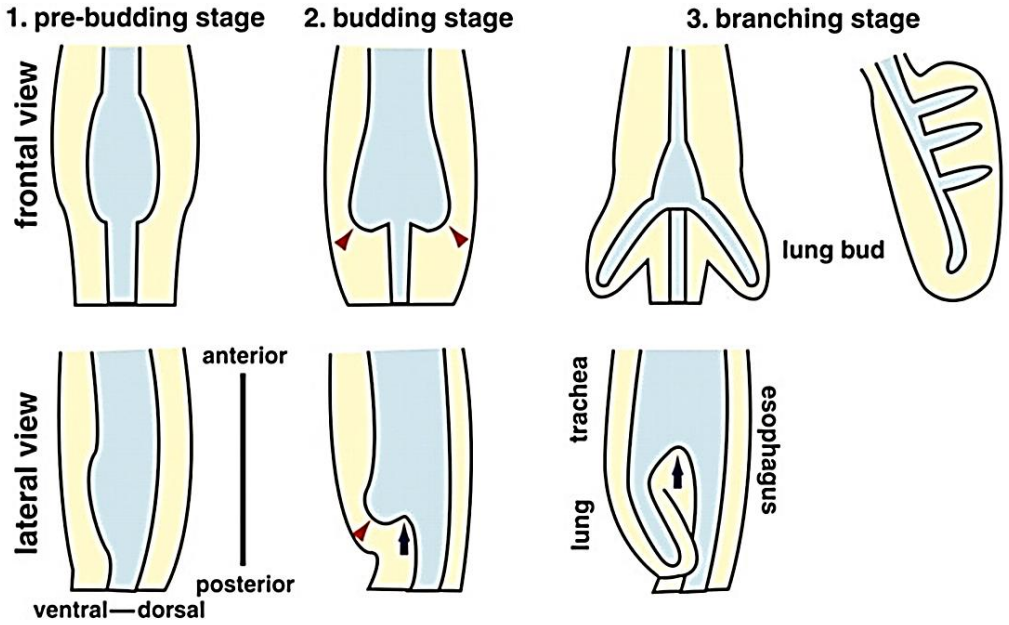

Figure 2 – Schematic representation of chick embryonic respiratory tract development. Adapted from Sakiyama *et al.*, 2003.

The initial stages of the chick lung development can be classified according to the number of secondary buds formed: b1, b2, or b3 stage, with one, two, or three secondary buds, respectively (Moura and Correia-Pinto, 2017). Later, secondary bronchi will sprout laterally, and tertiary bronchi (parabronchi) are formed, which will then anastomose and connect to the secondary bronchi (Maina, 2003). The chick adult lung consists of the parabronchial tree, responsible for gas exchange through interaction with blood capillaries, and the air sacs, a cystic-like structure involved in controlling air movement (Maina, 2003; Moura and Correia-Pinto, 2017).

1.5.2 Branching morphogenesis

Branching morphogenesis is characterized by sequential splitting of the airway epithelium into the surrounding mesenchyme; each lung bud undergoes a coordinated process of outgrowth, elongation, and bifurcation, giving rise to the respiratory airways. Branching morphogenesis is highly regulated by a network of signaling pathways that act through epithelial-mesenchymal interactions, such as Fibroblast Growth Factor (FGF), Sonic Hedgehog (SHH), Wingless-related Integration Site (WNT), among others.

FGF signaling is extremely important for branching morphogenesis, as *in vitro* inhibition of FGF signaling in the chick lung induced abnormal lung growth, with cystic structures of the secondary buds, a decrease in branching, and a disruption of the mesenchymal tissue (Moura *et al.*, 2011). Similarly, in the mouse model, *fgf10* knockout mice failed to develop lungs, resulting in death at birth (Sekine *et al.*, 1999). *fgf10* is expressed in the distal lung mesenchyme of chick lung; it stimulates distal epithelial growth by acting in the adjacent epithelium, where its specific cell surface receptor (FGF2R) is expressed (Moura *et al.*, 2011). *fgf2r* activation leads to the expression of *shh*, *spry2* (Sprouty 2) and *bmp4*, which will regulate the process of bud formation. *spry2* is expressed in the epithelium and acts as negative feedback for *fgf10* expression, thus inhibiting lung outgrowth.

Additionally, *shh* is also expressed in the epithelium and its signaling cascade includes the cell surface transmembrane receptor patched (*ptch*) and G protein-coupled transmembrane spanning protein smoothened (*smo*). In the absence of SHH, PTCH binds to SMO, suppressing its activity. However, when *shh* is expressed, it binds to *ptch*, which in turn activates *smo*, triggering the expression of glioblastoma (GLI) zinc finger transcription factor, resulting in the inhibition of *fgf10* expression (Fernandes-Silva *et al.*, 2017). While SHH is expressed in the epithelium, PTCH, SMO and GLI are present in the mesenchyme of the embryonic lung, eliciting epithelial-mesenchymal interactions occurring in SHH signaling. Accordingly, SHH signaling pathway restricts *fgf10* expression to the mesenchyme distal tip of lung buds; it inhibits its expression in the interbud region, promoting the bifurcation of the distal tip, establishing a new bud (Moura *et al.*, 2016). At branch tips, *shh* is suppressed by *hhip* (hedgehog-interacting protein) expression, allowing *fgf10* mesenchymal expression and, consequently, lung bud outgrowth. Moreover, *fgf10* also stimulates *shh* expression in a negative feedback loop that regulates bud formation. This interaction between *fgf10* and *shh* in a temporal-spatial manner is particularly important for branching morphogenesis, contributing to developing a fully functional organ.

WNT signaling also plays an important role during lung branching morphogenesis process. Canonical WNT ligands in both epithelium and mesenchyme, bind to the Frizzled (FZD) transmembrane receptors, thus stabilizing β-catenin in the cytoplasm and leading to its accumulation in the nucleus (Aros

et al., 2021). Once in the nucleus, β-catenin interacts with different transcription factors, activating the transcription of several downstream targets of WNT signaling pathway (Aros *et al.*, 2021). In particular, *wnt7b* is expressed throughout all pulmonary epithelium, specifically in the distal tips and secondary buds; it is associated with proper lung mesenchymal proliferation and differentiation and vascular development (Moura *et al.*, 2014). In fact, *wnt7b* knockout mice exhibited lung hypoplasia due to defects in early mesenchymal proliferation, resulting in respiratory failure and perinatal death (Shu *et al.*, 2002). Moreover, *wnt2/wnt2b* are both important at earlier stages during endodermal specification, by promoting *nkx2.1* expression (Aros *et al.*, 2021).

Furthermore, other transcription factors are involved in this complex process of early lung organogenesis, such as *sox2* and *sox9*, which determine the proximal-distal patterning of the respiratory airways. Regarding the chick lung, *sox2* is expressed in the epithelium of primary bronchus, except for the distal tips, being associated with proximal epithelium expression (Fernandes-Silva, Vaz-Cunha, *et al.*, 2017). Conversely, *sox9* has been associated with distal epithelium expression, as it is mainly expressed in the epithelium of secondary bronchi, and in the distal epithelial tips of the lung (Fernandes-Silva, Vaz-Cunha, *et al.*, 2017). Thus, the spatial distribution of *sox2* and *sox9* is most likely involved in controlling the proliferation and differentiation of proximal and distal airways, respectively, as it occurs with the mammalian lung (Zhu *et al.*, 2012).

Other numerous signaling pathways are also involved in lung organogenesis, and the interplay between them results in the formation of a fully functional organ. **Figure 3** shows a schematic representation of some of the signaling pathways involved in mammalian lung branching morphogenesis and its epithelial-mesenchymal interactions, which overall matches with the events underlying embryonic chick lung development.

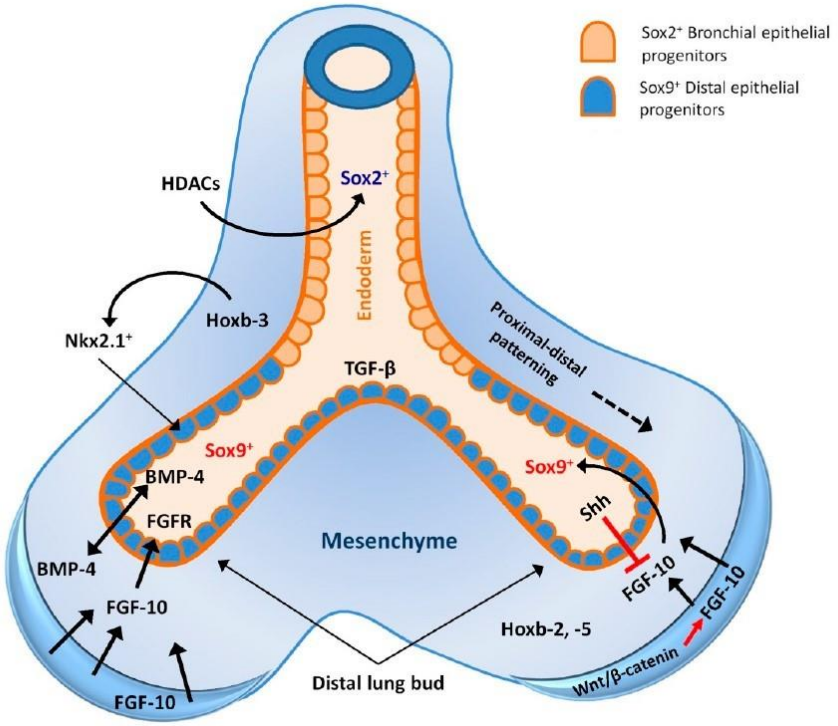

Figure 3 - Overview of molecular signaling pathways during lung branching morphogenesis and its epithelial-mesenchymal interactions. Adapted from Akram *et al.*, 2016.

1.6 Metabolism and embryonic development

In recent years, metabolism has emerged as a new player during embryonic development beyond its canonical function. It has been linked to several biological and cellular processes, such as cell signaling, differentiation, and proliferation during embryonic development (Miyazawa and Aulehla, 2018). As an example, it has been uncovered a non-canonical role of glucose metabolism during the early stages of embryo development.

Several studies have shown that metabolism is regulated both in time and space, and its functions can be distinguished in bioenergetic and metabolic signaling functions (**Fig. 4**). The bioenergetic function comprises the canonical activity needed to produce energy and biomass depending on the metabolic requirements of the tissue/cells, which can change over time. On the other hand, metabolic signaling function is associated with metabolites which play a role as rate-limiting factors, resulting in epigenetic and/or protein post-translational modifications (Miyazawa and Aulehla, 2018). For instance, it has been described that increased levels of acetyl-CoA, an important metabolite involved in energy production in mitochondria, induces histone acetylation at growth-related genes, enhancing transcription and consequently, cell growth and proliferation (Cai *et al.*, 2011). Moreover, non-metabolic moonlight

functions of metabolic enzymes and metabolites have been recently described, which are related to the nuclear roles of glycolytic enzymes in signaling or gene expression regulation (Miyazawa and Aulehla, 2018). For instance, the pyruvate kinase PKM2 isoform, which converts phosphoenolpyruvate (PEP) into pyruvate, induces the flux of glycolytic intermediates into the pentose phosphate pathway and one-carbon metabolism to answer the metabolic requirements of biomass production. However, PKM2 can also be translocated to the nucleus by epidermal growth factor (EGF) stimulation, where it interacts with β-catenin, leading to the transcription of cyclin D1 and *Myc,* promoting cell cycle progression (Boukouris *et al.*, 2016).

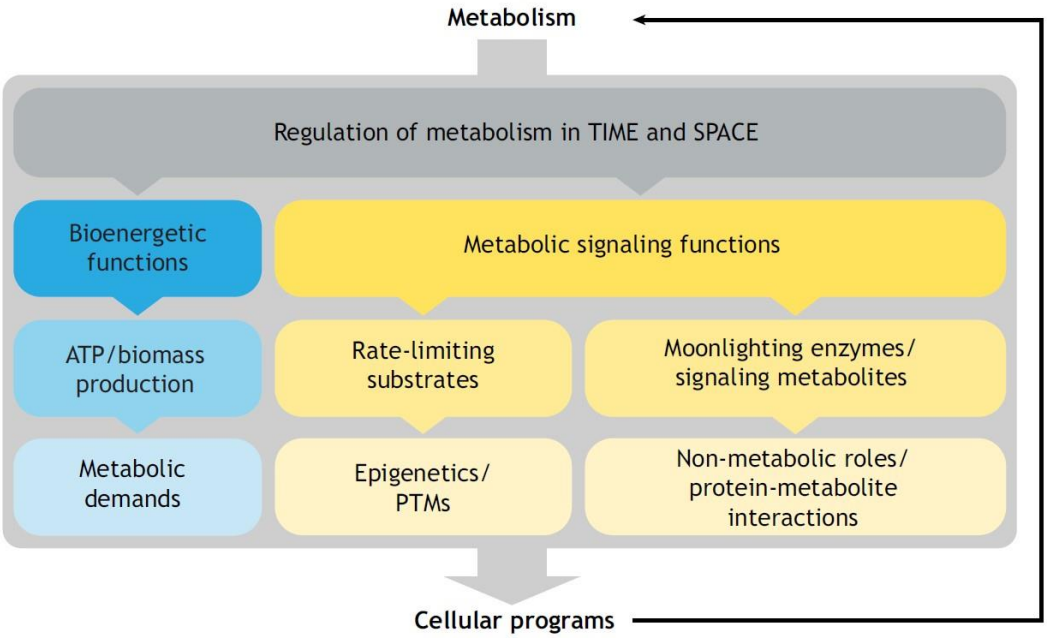

Figure 4 – Representation of the different functions of metabolism and its respective roles. Adapted from Miyazawa *et al.*, 2018.

Glycolytic metabolism plays an important role during embryonic development, and aerobic glycolysis is required in cells with high proliferative rates instead of oxidative phosphorylation, resembling the Warburg effect that occurs in cancer cells (Gándara and Wappner, 2018). Recent studies have shown the presence of a glycolytic activity gradient in mouse presomitic mesoderm (PSM). Cells present in the posterior region of the PSM, which are more undifferentiated, displayed higher aerobic glycolytic activity than the cells in the most anterior (differentiated) region (Bulusu *et al.*, 2017). This study highlights the importance of spatiotemporal metabolic changes throughout PSM development and differentiation. Furthermore, a relationship between signaling and metabolic gradients was also described in the PSM of the chicken embryo (Oginuma *et al.*, 2017). It is known that FGF and WNT signaling exhibit a gradient activity within the PSM, which controls somite formation and PSM patterning and differentiation. Recently,

a glycolytic gradient linked to the FGF/WNT signaling gradient has been described. Briefly, FGF signaling induces transcription of several glycolytic enzymes, creating a glycolytic gradient, increasing WNT signaling activity, controlling PSM development in the chicken embryo (Oginuma *et al.*, 2017).

Regarding the embryonic lung, the molecular mechanisms underlying early pulmonary development are quite well known; however, still little is known about the metabolic requirements of the embryonic lung. Glucose has been considered a major energy source for the mammalian adult lung through the uptake and catabolism of glucose (Liu and Summer, 2019).

Recent studies have shown that embryonic chicken lung adapts to a glycolytic lactate-based metabolic profile, which seems to be important in early lung branching morphogenesis (Fernandes-Silva *et al.*, 2021). This study shows that, at the beginning of lung branching morphogenesis process, glucose consumption is higher, and it decreases as branching proceeds, suggesting the contribution of other nutrients to sustain high proliferative rates. Moreover, lactate production increased with the increase of lung branching, which can be related to the need to obtain fast energy in high proliferative systems associated with organ growth and development. Total lactate dehydrogenase (LDH) levels also increased with branching, which may account for the observed lactate levels. Furthermore, a constant oxygen consumption rate was detected throughout branching, suggesting that the embryonic lung favors glycolytic metabolism rather than oxidative phosphorylation.

The crosstalk between molecular signaling pathways and metabolism appears to be crucial for normal organ development. Maternal hyperglycemia exposure during early pregnancy can alter the embryonic metabolic profile and impair proper lung organogenesis. However, these alterations and the underlying mechanisms are still poorly understood.

In this sense, this project aims to study the effect of high glucose levels in early lung branching morphogenesis, using *in vitro* chick lung explants exposed to different glucose concentrations. In this work, we analyzed signaling and metabolic players to determine the molecular mechanisms contributing to hyperglycemia-related pulmonary phenotype and that may account for the adverse effects of hyperglycemia on lung development.

2. Aims

Diabetes in pregnancy has been shown to affect the development of several organs, although its effect on early lung organogenesis remains poorly understood. In this sense, the main goal of this project is to characterize the impact of hyperglycemia in branching morphogenesis using the embryonic chick model.

Accordingly, *in vitro* chick lung explants were exposed to high glucose levels, and the impact on the signaling pathways underlying early lung events, such as patterning and branching, were assessed by *in situ* hybridization and qPCR. Additionally, glucose catabolic machinery and hormonal components were evaluated by *in situ* hybridization and qPCR in hyperglycemia-exposed lungs. Overall, this project aims to bring new insights into the mechanisms triggering hyperglycemic congenital abnormalities, unveiling glucose teratogenic potential in lung development.

The specific aims of this project are as follows:

1. Characterize the impact of hyperglycemia in the developing chick lung at the morphological level.

2. Identify hyperglycemia-induced alterations in the molecular mechanisms underlying lung patterning and branching.

3. Assess the impact of hyperglycemia in glucose catabolism-related genes to uncover metabolic alterations.

5. Determine insulin-related hormonal response induced by high glucose levels exposure.

3. Material and Methods

3.1. Ethical Statement

This work was carried out using the chicken embryo model (*Gallus gallus*) at early developmental stages. According to the Directive 2010/63/EU of the European Parliament and of the Council of 22 September 2010 on the protection of animals used for scientific purposes, the use of fertilized chicken eggs does not require ethical approval from the review board institution or the ethical committee. Furthermore, the Portuguese Directive 113/2013 of 7 August 2013 does not contain restrictions on the use of non-mammalian embryos.

3.2. Tissue Collection

Fertilized chicken eggs, *Gallus gallus*, obtained from commercial sources, were incubated for 4.5 to 5.5 days in a 49% humidified atmosphere at 37°C (Termaks KB400, Norway). Embryos were dissected under a stereomicroscope (Olympus SZX16, Japan), and embryonic chick lungs were collected and classified as b1, b2, or b3, according to the number of secondary buds formed: 1, 2, or 3, respectively. Lungs were then processed for *in vitro* lung explant culture or *in situ* hybridization. Embryos were also collected and staged according to HH stages (Hamburger and Hamilton, 1951) and processed for *in situ* hybridization.

3.3. *In vitro* lung explant culture

Embryonic chick lungs were dissected in PBS (8.0% NaCl, 0.2% KCl, 0.2% KH_2PO_4, 1.2% $Na_2HPO_4 \cdot H_2O$; pH 7.2-7.4) and b2 stage lungs were collected for *in vitro* lung explant culture (Moura, 2019). After dissection, lungs were transferred to nucleopore polycarbonate membranes with 8 µm pore size (Whatman, USA) in 24-well culture plates.

Membranes were presoaked in 400 µL of medium 199 (5.5 mM glucose; Sigma, USA) for at least 1 hour, at room temperature, before the lungs were placed in the membranes. Lung explants were then incubated with 200 µL of medium 199 with 5% heat-inactivated fetal calf serum (Invitrogen, USA), 10% chicken serum (Invitrogen), 1% L-glutamine (Invitrogen), 0.25 mg/mL ascorbic acid (Sigma) and 1% penicillin 5000 IU/mL combined with streptomycin 5000 IU/mL (Invitrogen), for 1 hour at 37°C in a 5% CO_2 incubator. Afterwards, explants were randomly assigned to one of four experimental groups and

exposed to medium with different D-glucose concentrations: control (5.5 mM), 25 mM, 50 mM, or 75 mM. Explants were incubated for 48h at 37°C in a 5% CO_2 incubator, and the corresponding medium was replaced at 24h of culture. At the end of the culture, explants were fixed overnight at 4°C in a 4% formaldehyde solution with 2 mM EGTA in PBS (pH 7.5) and processed for *in situ* hybridization or snap frozen in liquid nitrogen and stored at -80°C for RNA extraction.

3.4. Morphometric and Branching analysis

Chick lung explants were photographed at 0h (D0), 24h (D1), and 48h (D2) with a camera (Olympus U-LH100HG) coupled to a stereomicroscope (Olympus SZX16). At D0 and D2, the total number of peripheral airway buds was determined for the branching analysis. Moreover, regarding the morphometric analysis, the epithelial area and perimeter, and total area of the lung were also assessed at D0 and D2 using AxioVision Rel. 4.8 software (Carl Zeiss GmbH, Germany). Morphometric and branching results were expressed as D2/D0 ratio.

3.5. Whole mount *in situ* hybridization

In situ hybridization is a semi-quantitative technique that allows us to detect and determine the spatial distribution of a specific mRNA sequence in cells, tissue sections, or in the entire tissue (whole mount *in situ* hybridization). This technique is based on the complementarity between the nucleotide sequence of interest and an antisense RNA probe, establishing a stable hybrid. The RNA probe is usually labeled with digoxigenin (DIG), which will be recognized by an anti-DIG antibody conjugated with alkaline phosphatase. When the substrates are added, a purple precipitate is formed in the areas where the RNA probe is present.

3.5.1. RNA probe synthesis

3.5.1.1. Cloning protocol

Total RNA from an HH24 chicken embryo was extracted using TripleXtractor directRNA kit (Grisp, Portugal) according to the manufacturer's instructions. RNA concentration was determined using Nanodrop 1000 Spectrophotometer (Thermo Fisher Scientific, USA). Subsequently, 1 µg of RNA was treated with DNase I (Thermo Fisher Scientific) and reversely transcribed with GRS cDNA Synthesis kit (Grisp) to obtain cDNA. Briefly, RNA DNase-treated was mixed with dNTP mix and oligodT, and the

samples were heated at 65°C for 5 minutes to remove secondary RNA structures, followed by 2 minutes of incubation on ice. Next, reaction buffer 5x, Xpert RTase, and RNase inhibitor were added, and samples were first heated at 50°C for 50 minutes and then at 85°C for 5 minutes to inactivate the enzyme. Lastly, cDNA samples were stored at -20°C.

Specific primers for chicken *igf1r*, *igf2r* and *insr* (**Table 1**) were designed using NCBI primer design tool (https://www.ncbi.nlm.nih.gov/tools/primer-blast/). Primers were subsequently tested in conventional PCR, using NZY Taq 2x Green Master Mix (NZYTech, Portugal) and cDNA from chicken embryo as a template. PCR fragments were then cloned into the pCR™II-TOPO® vector (TOPO TA Cloning Kit, Invitrogen) using 4 µl of the PCR product, 1 µl of the TOPO vector and 1 µl of salt solution, followed by incubation at room temperature for at least 1 hour. Afterwards, the recombinant vectors were transformed into competent *E. coli* cells (NZYTech), plated in solid medium (LB/Ampicillin/IPTG/X-Gal) and incubated overnight at 37°C. Subsequently, isolated white colonies were inoculated in LB (Luria-Bertani) liquid medium plus ampicillin, overnight at 37°C, 200 rpm. Plasmid DNA was then extracted using Genejet Plasmid Miniprep Kit (Thermo Fisher Scientific), and the presence of the fragment of interest was determined by conventional PCR and M13 plasmid universal primers. Afterwards, PCR products were analyzed in a 1% agarose gel and the expected size of the fragments was confirmed by comparison with a DNA molecular weight ladder (GRS Universal Ladder). Plasmid DNA with the correct insert size was sequenced (GATC Biotech, Germany) and the fragment orientation was determined.

To obtain enough DNA template for the *in vitro* transcription step, DNA containing the fragments of interest were then amplified by PCR using 500 ng of plasmid DNA and M13 plasmid universal primers. Afterwards, PCR products were analyzed in a 1% agarose gel. Subsequently, the DNA bands were excised from the agarose gel and DNA was isolated and purified using GRS PCR and Gel Band Purification Kit (Grisp), following the manufacturer's instructions. DNA concentration was determined using Nanodrop Spectrophotometer and DNA was stored at -20°C. Plasmid DNA for *sox2* (Dady *et al.*, 2012) and *sox9* (Domowicz *et al.*, 2011) was already available in the lab.

Table 1 - Primer sequences forward (Fw) and reverse (Rv) used for *in situ* hybridization and its annealing temperature and fragment expected size.

Gene	Access number	Sequence 5'-3'	Annealing T (ºC)	Expected size (bp)
igf1r	NM_205032.2	Fw – CAGTTCTCTCCTTGCCATCC Rv - CAGCATCCAACTCCTCTTCC	57.7	513
igf2r	NM_204970.1	Fw – ACAGCAGGCACAGAACTCTAC Rv – TGCTGACAAACTGGGCTGTA	58	925
insr	XM_040692955.1	Fw – AGTCCTTCCTAACGCCTCCT Rv – AGACCAAACAATCCCCCGAA	59.4	970
*ldha**	NM_205284.2	Fw – GCACTTTCCAAGTAGGTCAAATCC Rv – AGTCTTTGGTTTCACGTTGTGT	59.7	292
*ldhb**	NM_204177.3	Fw – GCAGGTTGTTGAAAGTGCCT Rv – AGTGAGTAGAGAGCCCACAT	56.1	374

* Fernandes-Silva *et al.*, 2021

3.5.1.2. ***In vitro* transcription**

Antisense digoxigenin-labeled RNA probes for *igf1r, igf2r, insr, ldha, ldhb, sox2 and sox9* were synthetized by an *in vitro* transcription reaction. For this purpose, 750 ng of DNA resulting from gel band purification was used as a template and mixed with dithiothreitol (DTT), DIG RNA labeling mix (Roche, Germany), transcription buffer (5x or 10x, depending on the RNA polymerase), ribonuclease inhibitor (RNasin; NZYTech) and RNA polymerase (according to fragment orientation in the plasmid; **Table 2**), following manufacturer's instructions. This reaction mix was incubated at 37°C for 3h, and after this period, probe synthesis was verified in a 0.8% agarose gel. Subsequently, DNase I (Thermo Fischer Scientific) and RNasin were added to the mixture on ice, followed by incubation at 37°C for 30 minutes. Then, the RNA probes were precipitated with Tris-EDTA (TE), lithium chloride 4M (LiCl), and ethanol 100% and incubated at -80°C for 45 minutes, protected from light. Afterwards, samples were centrifuged at 14000 rpm for 30 minutes at 4°C, and the supernatant was discarded. The pellet was washed with ethanol 70% and centrifuged again at 14000 rpm for 15 minutes at 4°C. Then, the supernatant was discarded, and the pellet was resuspended in 50 µl of EDTA 10 mM. Probe synthesis was verified in a 0.8% agarose gel at the end of the protocol. RNA probes were stored at -20°C until they were used for *in situ* hybridization.

Table 3 - RNA polymerase and the corresponding supplier and transcription buffer used for *in vitro* transcription during RNA probe synthesis for each gene.

Gene	RNA polymerase	Supplier	Transcription Buffer
igf1r	T7	Promega	5x
igf2r	Sp6	Roche	10x
insr	T7	Promega	5x
ldha	Sp6	Roche	10x
ldhb	Sp6	Roche	10x
sox2	T7	Promega	5x
sox9	T7	Promega	5x

3.5.2. *In situ* hybridization protocol

Lungs and embryos were fixed in a 4% formaldehyde solution with 2 mM EGTA in PBS (pH 7.5) at 4°C overnight. Tissues were then washed in PBT (PBS, 0.1% Tween 20), followed by dehydration in methanol, and stored at -20°C. Whole mount *in situ* hybridization was performed as previously described (Moura, 2019). Tissues were first rehydrated through a methanol/PBT series: methanol/PBT (75:25), methanol/PBT (50:50), and methanol/PBT (25/75); and finally washed in PBT. To permeabilize the cell membrane, tissues were then incubated with a 0.05% proteinase K (Roche) solution in PBT, for exactly 2 minutes for the lungs and 35 minutes for the HH24 embryos, and then washed with PBT. Lungs and embryos were then incubated with a post-fixing solution (10% formaldehyde and 0.4% glutaraldehyde in PBT) for at least 20 minutes and washed again with PBT. Subsequently, tissues were incubated with PBT and hybridization solution (50:50) (0.5% CHAPS, 50% formamide, 6.5% SSC, 1% EDTA 0.5 M, 0.2% Tween 20, 0.25% t-RNA, 0.2% heparin) and then incubated with hybridization solution at 70°C for at least 1h. Next, tissues were incubated with specific antisense DIG-labeled RNA probes previously synthetized, diluted in hybridization solution, at 70°C overnight. On the next day, washes with pre-warmed hybridization solution were performed to remove the probe, and afterwards, tissues were washed first in hybridization solution with MABT (50:50) (5.8% $C_4H_4O_4$, 4.4% NaCl, 7% NaOH, 1% Tween 20, pH 7.5) and then twice

with MABT. Later, tissues were incubated with 20% blocking reagent (Roche) in MABT, followed by incubation with 20% blocking reagent and 20% goat serum (Invitrogen) in MABT. Next, tissues were incubated overnight with MABT, 20% blocking reagent, 20% goat serum and 1:2000 anti-DIG antibody (Roche) at room temperature. Several washes with MABT were performed the next day to remove the antibody and tissues were incubated overnight with MABT at room temperature. On the last day, tissues were washed with NTMT solution (0.1 M NaCl, 0.1 M Tris–HCl, 50 mM $MgCl_2$, 1% Tween 20) and lastly, tissues were incubated with a developing solution consisting of NTMT with NBT (Roche) and BCIP (Roche), at 37°C protected from light. The developing reaction was stopped simultaneously for all experimental groups incubated with the same probe by washing with PBT. All lungs and embryos were photographed using a camera (Olympus U-LH100HG) coupled to a stereomicroscope (Olympus SZX16) and stored in PBT/0.1% azide at 4°C.

3.6. Histological Sections

Hybridized chicken lungs were dehydrated through a series of ethanol solutions (70%, 96% and 100% ethanol) and embedded in a 2-hydroxyethyl methacrylate solution (Heraeus Kulzer, Germany), followed by sectioning in 25 µm thick histological slides using a rotatory microtome (Leica RM 2155, Germany). Lung histological slides were photographed using a camera (Olympus DP70) coupled to a microscope (Olympus BX61).

3.7. Quantitative real-time PCR (qPCR)

Total RNA and cDNA from D2 chick lung explants were obtained as previously mentioned in section 4.1.1, with an alteration in the cDNA synthesis program, which was as follows: 1) 65°C for 5 minutes, 2) 50°C for 15 minutes, and 3) 85°C for 5 minutes. Specific exon-exon spanning primers were designed for *wnt7b* using the NCBI primer design tool (https://www.ncbi.nlm.nih.gov/tools/primer-blast/). Primers for *fgf10*, *shh* and *wnt7b* (**Table 3**) were first tested in conventional PCR and optimized for annealing temperature, using NZY Taq 2x Green Master Mix (NZYTech, Portugal) and cDNA from a pool of b2 stage lungs as a template. Subsequently, primers were also optimized for efficiency range. Primers for *glut1*, *glut3*, *hk1*, *pfk1*, and housekeeping *actin-β* (**Table 3**) were already validated and available in the lab. qPCR was performed in duplicate (n ≥ 6 per condition) with the SYBR method according to the manufacturer's instructions, using NZYSupreme qPCR Green Master Mix (2x) ROX (NZYTech) and 1 µl of 1:6 diluted cDNA. The qPCR program was as follows: 1) polymerase activation at 95ºC for 2 min; 2)

amplification in 40 cycles (denaturation at 95ºC, for 5 secs; combined annealing/extension at the appropriate annealing temperature, for 30 sec), using 7500 Fast Real-Time PCR System Applied Biosystems equipment. Data on gene expression was first normalized for the housekeeping *actin-β*, and relative expression was calculated following the mathematical model $2^{(-\Delta Ct)}$ (Livak and Schmittgen, 2001).

Table 4 - Primer sequences forward (Fw) and reverse (Rv) used for qPCR and its annealing temperatures and fragment expected size.

Gene	Access number	Sequence 5'-3'	Annealing T (ºC)	Expected size (bp)
*actin-β**	NM_205518.2	Fw – CTTCTAAACCGGACTGTTACCA Rv – AAACAAATAAAGCCATGCCAATCT	58	100
*fgf10***	NM_204696.2	Fw – GAGAAGAACGGCAAGGTCAG Rv – AACTGCCACAACTCCAATTTC	58	93
*shh****	NM_204821.1	Fw – GCTGACAGACTGATGACTCA Rv - TCGTAGTGCAGCGATTCCTC	58	146
wnt7b	XM_046908560.1	Fw – TGCACGAAGGCTGATGAACT Rv - TCTACTGGCTCGTACCACCT	58	211
*glut1**	NM_205209.2	Fw – GCAGTTCGGCTACAACACCG Rv – ATCAGCATGGAGTTACGCCG	58	222
*glut3**	NM_205511.2	Fw – GTACCGTTCGGGTTCCGTTAG Rv – AATGGCAGCAACAGAAACAGC	62	115
*hk1**	NM_204101.2	Fw – CTGGCCTACTACTTCACCGAG Rv – TCACTGTCGCTGTTGGGTTA	58	166
*pfk1**	NM_001396039.1	Fw - CGTGGGAGGAGCTTTGAGAA Rv - CAGCCCACCTCACGTATCTG	56	236

*Fernandes-Silva *et al.*, 2021, **Young *et al.*, 2019, ***Hu *et al.*, 2015

3.8. Statistical analysis

Statistical analysis was performed using GraphPad Prism software. Normal distribution of the variables was tested using the Shapiro-Wilk test. One-Way ANOVA test was performed, followed by Fisher's Least Significant Difference (LSD) post hoc test for multiple comparisons. All quantitative data were presented as mean ± standard deviation (SD), and statistical significance was set at $p < 0.05$.

4. Results

4.1. Impact of hyperglycemia on lung branching and growth

To study the impact of abnormal high glucose levels on lung branching and growth, lung explant culture was performed. This *in vitro* approach allows studying the whole organ in controlled conditions, maintaining tissue interactions and structure comparable to *in vivo*. Specifically, lung explants were exposed to increasing doses of glucose (25, 50, and 75 mM) for 48 hours. These concentrations were based on *in vitro* studies using cell lines, where 25 mM of D-glucose was used to induce a hyperglycemic environment (Weiss *et al.*, 2001). Thus, we decided to use the same concentration and, since we were using the whole organ (a more complex system than cell lines) we also selected higher doses, such as 50 and 75 mM. Furthermore, other studies using a shell-less chicken embryo culture *in vitro* also have used similar and higher concentrations (Datar and Bhonde, 2005). As a control, explants were exposed to physiological levels of glucose (5.5 mM). **Figure 5** shows representative images of chick lung explants at D0 (**Fig. 5**a, c, e, g) and D2 (**Fig. 5**b, d, f, h) treated with different doses of glucose. It is possible to observe that explants exposed to 50 and 75 mM of glucose (**Fig. 5**f, h) look smaller than controls (**Fig. 5**b).

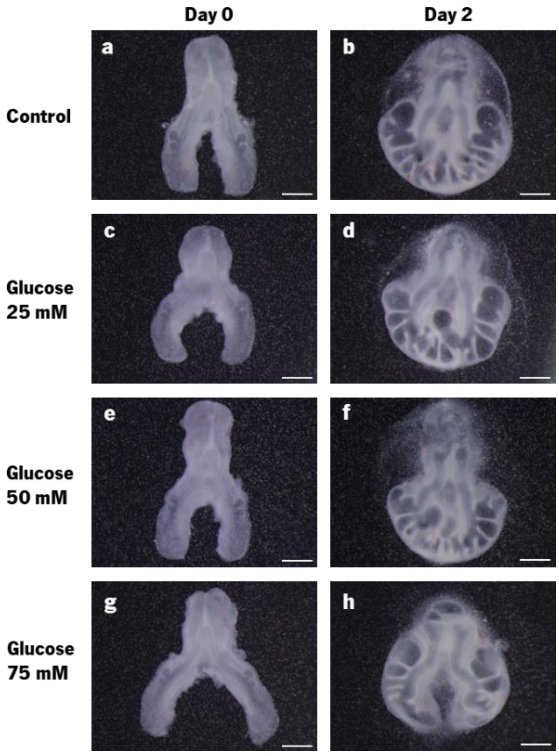

Figure 5 - *In vitro* chick lung explant culture exposed to different glucose concentrations. Representative examples of b2 stage lungs exposed to 5.5 mM (control) (**a, b**), 25 mM (**c, d**), 50 mM (**e, f**) and 75 mM (**g, h**) of glucose at D0 (**a, c, e, g**) and D2 (**b, d, f, h**) of culture. Scale bar: 500 µm; n ≥15 per condition.

To evaluate the influence of hyperglycemic conditions on lung growth, chick lung explants were morphometrically analyzed. On D0 and D2, the epithelial area and perimeter, and total area of the lung were assessed, and the results were expressed as D2/D0 ratio.

Regarding the total area of the lung (**Fig. 6**a), explants treated with 50 mM of glucose showed a statistically significant decrease when compared to controls (p<0.0001). Likewise, 75 mM-treated lungs also showed a significant decrease in the total area of the lung compared to controls (p=0.0018). Besides, no differences were observed between 50 and 75 mM-exposed lungs. On the other hand, 25 mM-exposed lungs did not display any differences compared to the controls. Nonetheless, 50 and 75 mM-exposed lungs displayed a statically significant decrease in the total area of the lung when compared to 25 mM dose (p<0.0001; p=0.0031).

Furthermore, the epithelial perimeter of glucose-treated lung explants was also evaluated (**Fig. 6**b). Similarly to the lung total area results, 50 and 75 mM-treated lungs exhibited decreased epithelial perimeter compared to the controls (p<0.0001; p<0.0001). Additionally, no differences were observed in the 25 mM dose. Lungs exposed to 50 and 75 mM of glucose showed a statistically significant decrease in the epithelial perimeter compared to the 25 mM dose (p<0.0001; p<0.0001); however, no differences were found between 50 mM and 75 mM-treated lung explants.

Regarding the lung epithelial area, explants treated with 50 and 75 mM of glucose displayed a statistically significant decrease in the epithelial area of the lung (**Fig. 6**c), when compared to the controls (p<0.0001; p=0.0018). Once again, no differences were found between 50 mM and 75 mM dose, nor in 25 mM dose compared to the controls. Lastly, 50 and 75 mM-treated lungs exhibited a decrease in the epithelial area compared to 25 mM-treated lungs (p<0.0001; p<0.0001). These results are in accordance with the results observed in both epithelial perimeter and total area of the lung, suggesting an impairment in lung growth due to high glucose levels exposure *in vitro*.

Lung branching was also evaluated in glucose-treated lung explants. Overall, branching analysis showed that high glucose levels result in decreased lung branching, indicated by the decrease in the number of secondary buds formed after 48 hours of culture. Chick lung explants treated with 50 mM and 75 mM of glucose showed a statistically significant reduction of branching compared to control explants (**Fig. 6**d; p=0.0103, p=0.032), similarly to morphometric results. Moreover, no differences were observed between the 25 mM dose and the controls, nor between 50 mM and 75 mM-treated lungs. Branching was also decreased in the 50 mM and 75 mM doses when compared to the 25 mM dose (p=0.0033; p=0.01118). Branching results are in accordance with the morphometric results, where a decrease in lung branching and growth is observed in the two highest doses of glucose.

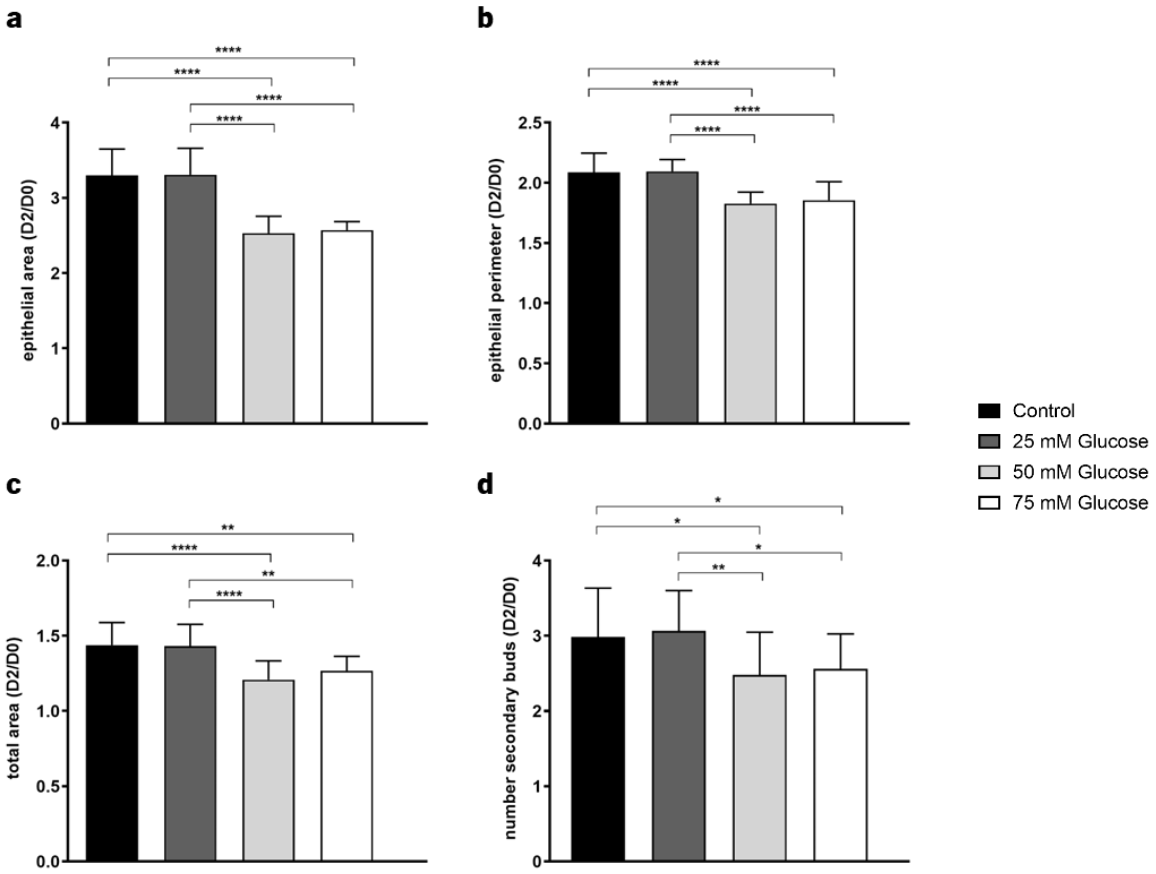

Figure 6 - Morphometric and branching analysis of chick lung explants exposed to 5.5 mM (control), 25 mM, 50 mM or 75 mM of glucose. At D0 and D2, the epithelial area (**a**) and perimeter (**b**), and total area (**c**) of the lung were determined, as well as the number of secondary buds formed (**d**). Results are expressed as D2/D0 ratio and represented as mean ± SD. Statistically significant results are presented as: * $p<0.05$, ** $p<0.01$ and **** $p<0.0001$. n ≥ 12 per condition.

4.2. Impact of hyperglycemia on insulin-related gene expression

Considering the impact of elevated glucose levels on lung branching and growth, we asked whether that could result from an impairment of Insulin/IGF system. The Insulin/IGF system is very important during embryonic development; it is known that this signaling impacts growth and development and is usually regulated by glucose. In this sense, the expression of *insr*, *igf1r* and *igf2r* was assessed by *in situ* hybridization, to further evaluate insulin-related gene expression after hyperglycemia exposure in lung explants. Since no information was available in the literature regarding the spatial distribution of these three receptors in the embryonic lung, their expression pattern was first characterized by *in situ* hybridization, using b1, b2, and b3 stage lungs. The probes for *insr*, *igf1r* and *igf2r* were designed and produced in-house (**Supplementary Figure 1,** Appendix I), and tested in whole embryos to assess its specificity (**Supplementary Figure 2**, Appendix I).

4.2.1. Characterization of the expression pattern of insulin and IGF receptors

Regarding *igf1r* expression, we can observe that *igf1r* is expressed throughout the lung epithelium, mostly in the secondary lung buds (**Fig. 7**b, asterisk), and in the most distal part of the main bronchi (**Fig. 7**a, black arrowhead). No expression was observed in the mesenchyme, and *igf1r* expression pattern is not altered between the three stages of lung development. Histological sections of hybridized lungs confirm the absence of *igf1r* mRNA in the mesenchyme and its presence in the epithelium compartment (**Fig. 7**d, e, f).

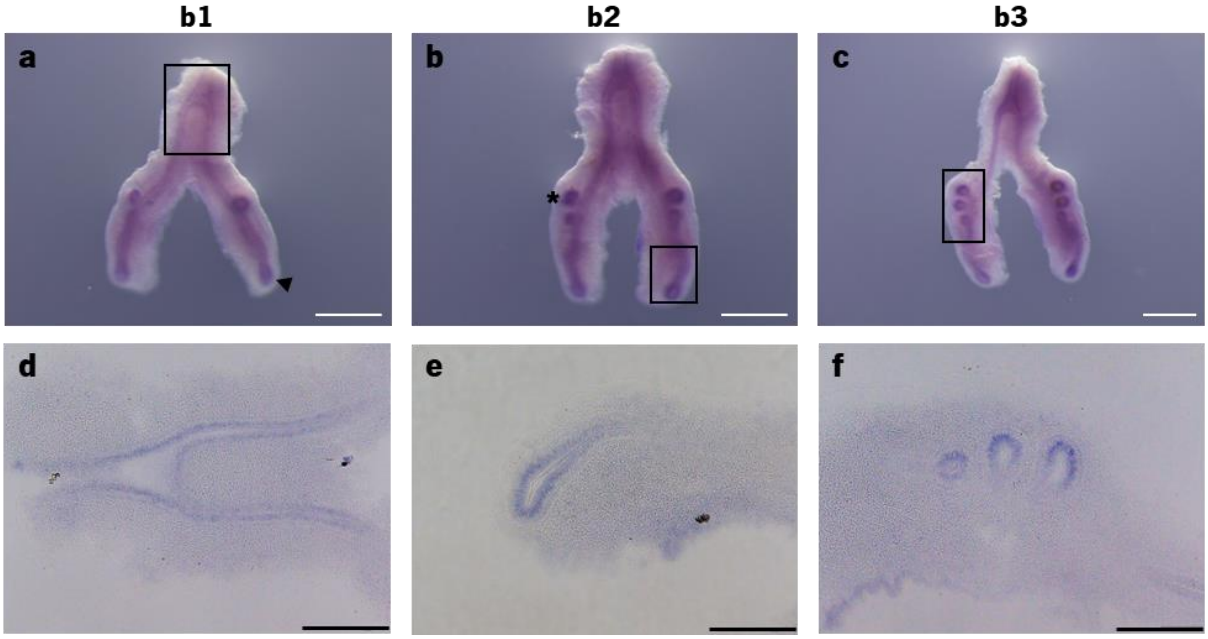

Figure 7 - Characterization of *igf1r* expression pattern during embryonic chick lung development. Representative examples of *in situ* hybridization of *igf1r* for b1 (**a**), b2 (**b**) and b3 (**c**) stage lungs. Black rectangles in images **a**, **b** and **c** represent the area shown in the corresponding histological section (**d**, **e** and **f**. Scale bar: a, b, c – 500 µm; d, e, f – 200 µm. n ≥ 16 per stage. Black arrowhead: distal epithelial region; Asterisk: secondary bronchi.

igf2r mRNA is also present in the main epithelial bronchi, particularly in the distal tips of the lung (**Fig. 8**a, black arrowhead) and also in the secondary bronchi (**Fig. 8**c, asterisk). There are no differences in *igf2r* expression between the three stages studied; slide sectioning confirmed this expression pattern (**Fig. 8**d, e, f).

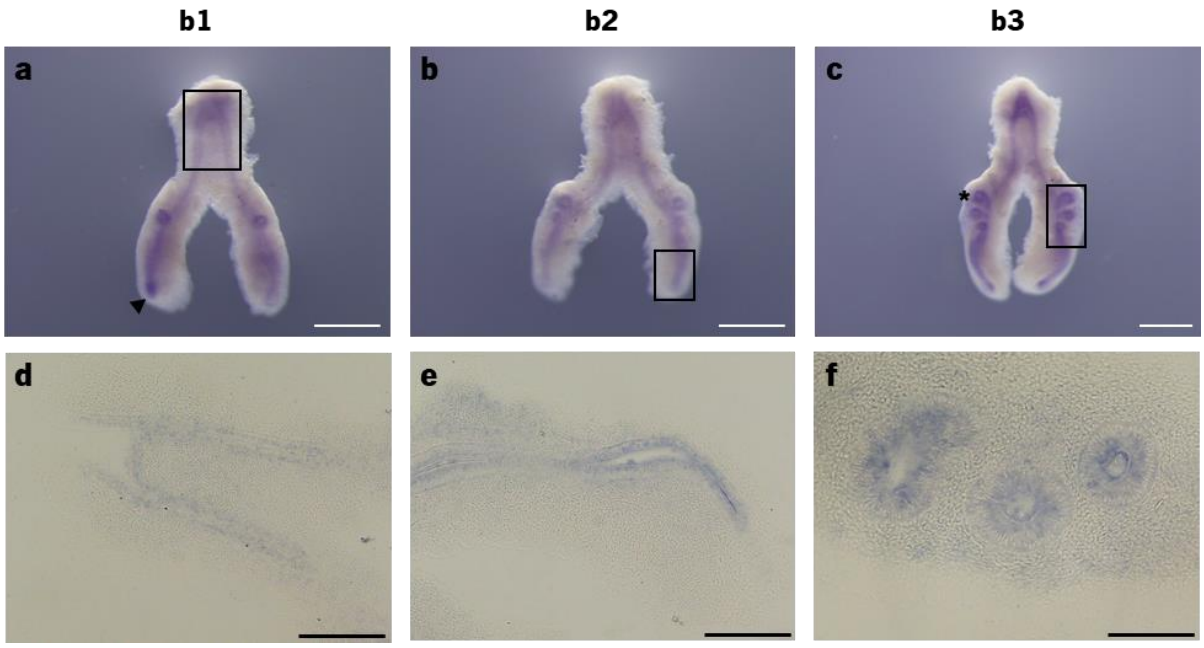

Figure 8 - Characterization of *igf2r* expression pattern during embryonic chick lung development. Representative examples of *in situ* hybridization of *igf2r* for b1 (**a**), b2 (**b**) and b3 (**c**) stage lungs. Black rectangles in images **a**, **b** and **c** represent the area shown in the corresponding histological section (**d**, **e**, and **f**). Scale bar: a, b, c – 500 µm; d, e – 200 µm; f – 100 µm. n ≥ 16 per stage. Black arrowhead: distal epithelial region; Asterisk: secondary bronchi.

insr is faintly expressed in the epithelium of secondary bronchi (**Fig. 9**c, asterisk) in the three stages of embryonic lung development, with a slight increase of expression in b3 stage. *insr* appears to be absent in the mesenchyme of the lung. It is worth mentioning that to obtain this weak expression, the lungs were left for more than 24 hours in the developing solution. Lung sectioning was not performed in this case as lower levels of expression would not be detected.

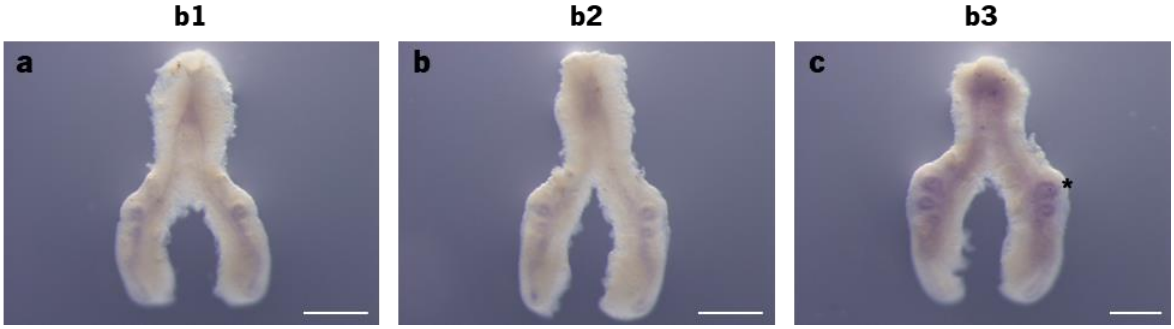

Figure 9 - Characterization of *insr* expression pattern during embryonic chick lung development. Representative examples of *in situ* hybridization for *insr* of b1 (**a**), b2 (**b**) and b3 (**c**) stage lungs. Scale bar: 500 µm. n ≥ 16 per stage. Asterisk: secondary bronchi.

4.2.2. Impact of high glucose levels in the expression of insulin and IGF receptors

After characterizing the expression pattern of *igf1r*, *igf2r* and *insr* in the embryonic chick lung, the expression of these three receptors was evaluated in chick lung explants exposed to 5.5 (control), 25, 50 or 75 mM of glucose (**Fig. 10**).

igf1r increases its expression in glucose-supplemented lung explants, especially in the 50 mM and 75 mM doses (**Fig. 10**a, b, c, d) compared to control. No alterations were observed in the expression of *igf2r* (**Fig. 10**e, f, g, h) and *insr* (**Fig. 10**i, j, k, l) in supplemented lung explants compared to the controls. Furthermore, the expression pattern observed in these three receptors in lung explants is in accordance with the characterization described previously (**Fig**. **7**, **8** and **9**).

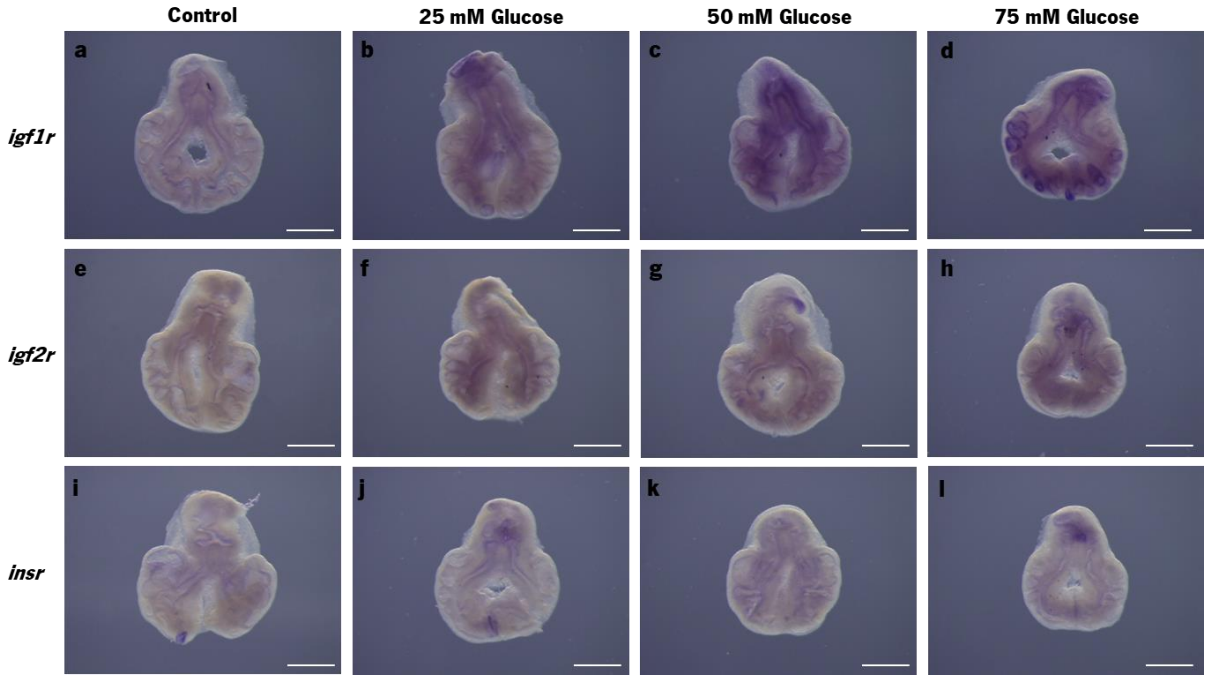

Figure 10 - *In vitro* chick lung explants supplemented with glucose, followed by *in situ* hybridization for *igf1r*, *igf2r* and *insr*. Representative examples of D2 chick lung explants treated with 5.5 mM (control) (**a**, **e**, **i**), 25 mM (**b**, **f** and **j**), 50 mM (**c**, **g**, **k**) and 75 mM (**d**, **h**, **l**) of glucose, probed for *igf1r* (**a**, **b**, **c**, **d**), *igf2r* (**e**, **f**, **g**, **h**) and *insr* (**i**, **j**, **k**, **l**). Scale bar: 500 µm. n ≥ 5 per condition.

4.3. Impact of hyperglycemia in key metabolic players

The crosstalk between metabolism and signaling is important for normal organ development. As hyperglycemia can impair glucose metabolism, we analyzed if there is any alteration in the expression of glucose-related key metabolic players, that could be associated with impaired lung growth and branching. Therefore, to determine the impact of hyperglycemia on the metabolic component of the embryonic lung, the expression levels of glucose catabolism-related enzymes (*hk1*, *pfk1*, *ldha* and *ldhb*) and glucose transporters (*glut1* and *glut3*) were assessed by *in situ* hybridization and qPCR in glucose treated explants. Since in the morphometric and branching analysis, no differences were observed between the 50 mM and 75 mM-treated explants, from this point onwards, only 25 mM and 50 Mm-exposed lungs were used.

Thus, *glut1*, *glut3*, *hk1* and *pfk1* expression levels were evaluated by qPCR, in chick lung explants exposed to 25 mM and 50 mM of glucose. *glut1* relative expression (**Fig. 11**a) decreased in both 25 mM and 50 mM-treated lungs when compared to control (p<0.0001; p<0.0001).

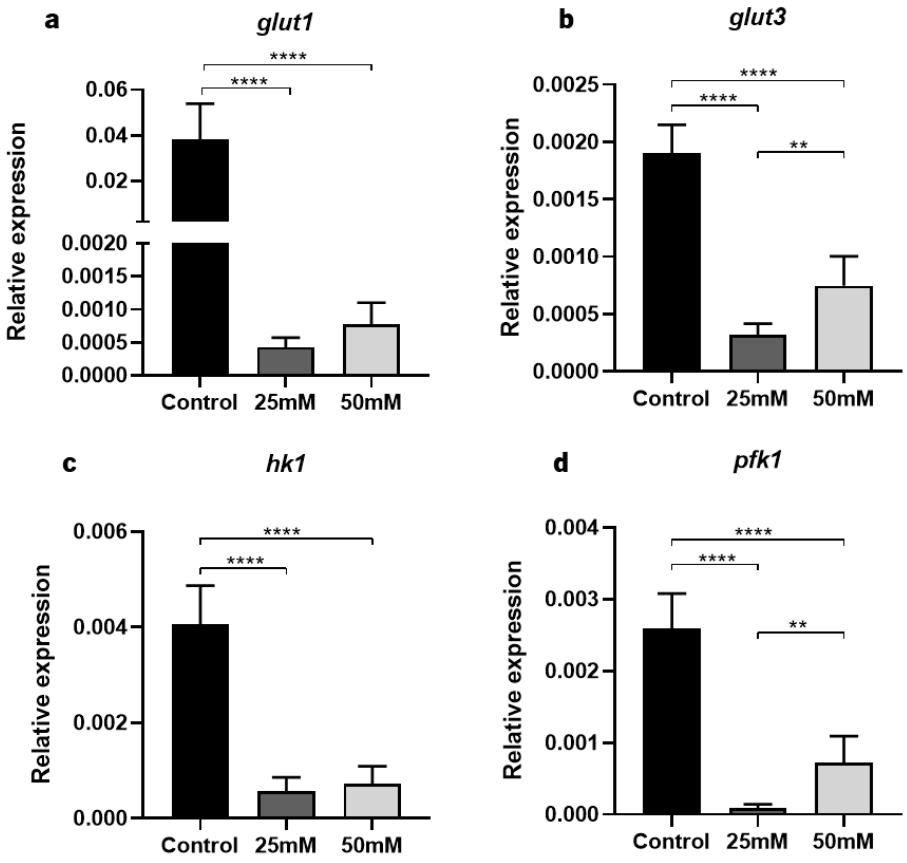

Figure 11 - mRNA expression levels of glucose transporters (*glut1* and *glut3*) and glucose catabolism related enzymes (*hk1* and *pfk1*) evaluated by qPCR. Relative expression of *glut1* (**a**), *glut3* (**b**), *hk1* (**c**) and *pfk1* (**d**) in D2 chick lungs explants treated with 5.5 mM (control), 25 mM and 50 mM of glucose. Data on gene expression was normalized for the housekeeping actin-β. Results are represented as mean ± SD. Statistically significant results are presented as: ** p<0.01 and **** p<0.0001. n ≥ 6 per condition.

Moreover, no differences were observed between 25 mM and 50 mM doses. *glut3* relative expression (**Fig. 11**b) showed a significant statistical decrease in 25 mM and 50 mM doses of glucose compared to controls (p<0.0001; p<0.0001). Additionally, *glut3* expression in 50 mM-exposed lungs is statistically significantly higher than in 25 mM-exposed lungs (p=0.0035).

Furthermore, *hk1* (**Fig. 11**c) exhibited decreased relative expression in 25 mM and 50 mM-treated lung explants compared to controls (p<0.0001; p<0.0001). Likewise, *pfk1* relative expression (**Fig. 11**d) showed a significant statistical decrease in 25 mM and 50 mM-treated lung explants when compared to controls (p<0.0001; p<0.0001). Similarly to what happens in *glut3* expression, explants treated with 50 mM of glucose showed higher *pfk1* relative expression compared to 25 mM dose (p=0.0074).

ldha and *ldhb* expression pattern was assessed by *in situ* hybridization in glucose-treated chick lung explants due to the specific spatial distribution of these genes in the embryonic lung already described in the literature (Fernandes-Silva *et al.*, 2021). *ldha* appears to be expressed in both epithelium and mesenchyme, and no differences in the expression is observed between experimental groups (**Fig. 12**a, b, c). *ldhb* increases its expression in glucose-supplemented lung explants, compared to the control, especially in the 50 mM dose (**Fig. 12**d, e, f). An increase in *ldhb* expression is observed in the secondary bronchi (**Fig. 12**f, asterisk) and the most distal region of the lung (**Fig. 12**f, white arrowhead), in glucose-treated lungs. In the three conditions studied, *ldhb* appears to have lower expression in the proximal region of the lung (**Fig. 8**d, black arrow).

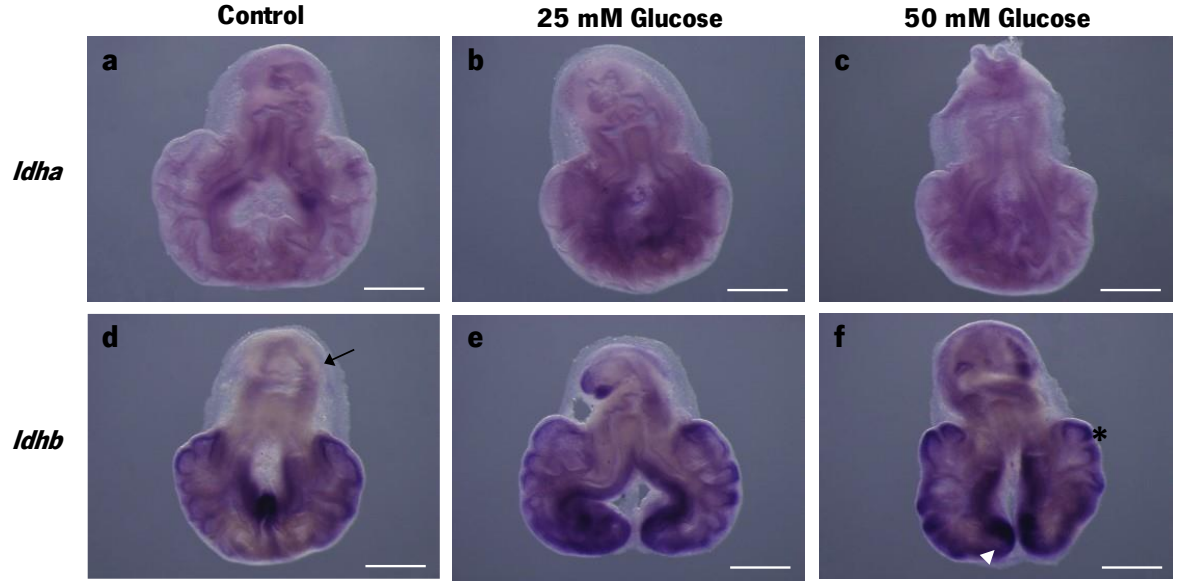

Figure 12 - *In vitro* chick lung explants supplemented with glucose, followed by *in situ* hybridization for *ldha* and *ldhb*. Representative examples of D2 chick lung explants supplemented with 5.5 mM (control) (**a** and **d**), 25 mM (**b** and **e**) and 50 mM (**c** and **f**) of glucose, probed for *ldha* (**a**, **b**, **c**) and *ldhb* (**d**, **e**, **f**). Scale bar: 500 µm. n ≥ 5 per condition. White arrowhead: distal epithelial region; Asterisk: secondary bronchi; Black arrow: proximal region of the lung.

4.4. Lung patterning and branching-related gene expression in hyperglycemia exposed lungs

To understand the mechanisms behind the morphometric and branching alterations observed in chick lung explants exposed to hyperglycemic conditions, we decided to further explore the molecular pathways involved in lung branching and patterning. Thus, the expression pattern/levels of genes involved in patterning (*sox2* and *sox9*) and branching (*fgf10*, *shh*, *wnt7b*) were evaluated by *in situ* hybridization and qPCR, respectively.

sox2 and *sox9* have a very particular expression pattern in the embryonic lung, with expression in the proximal and distal regions of the lung, respectively. Thus, these proximal-distal markers were evaluated by *in situ* hybridization, to understand whether their expression pattern is altered or not after hyperglycemic exposure. The results show that *sox2* expression pattern and levels appear to be conserved in glucose-supplemented lung explants compared to the controls (**Fig. 13**a, b, c). *sox2* is expressed in the epithelium of the main bronchi, especially in the most proximal region of the lung (**Fig. 13**a, b, c). *sox2* is not expressed in the secondary bronchi and it is less expressed in the distal tip of the lung. Moreover, *sox2* is not present in the mesenchymal compartment. Regarding *sox9*, its expression levels seem to be decreased in the distal region of 50 mM-exposed lung explants compared to control and 25 mM-exposed lungs (**Fig. 13**d, e, f). *sox9* is mainly expressed in the mesenchyme of the trachea region, and it appears to be absent in the epithelium, except for the secondary bronchi (**Fig. 13**d, e, f).

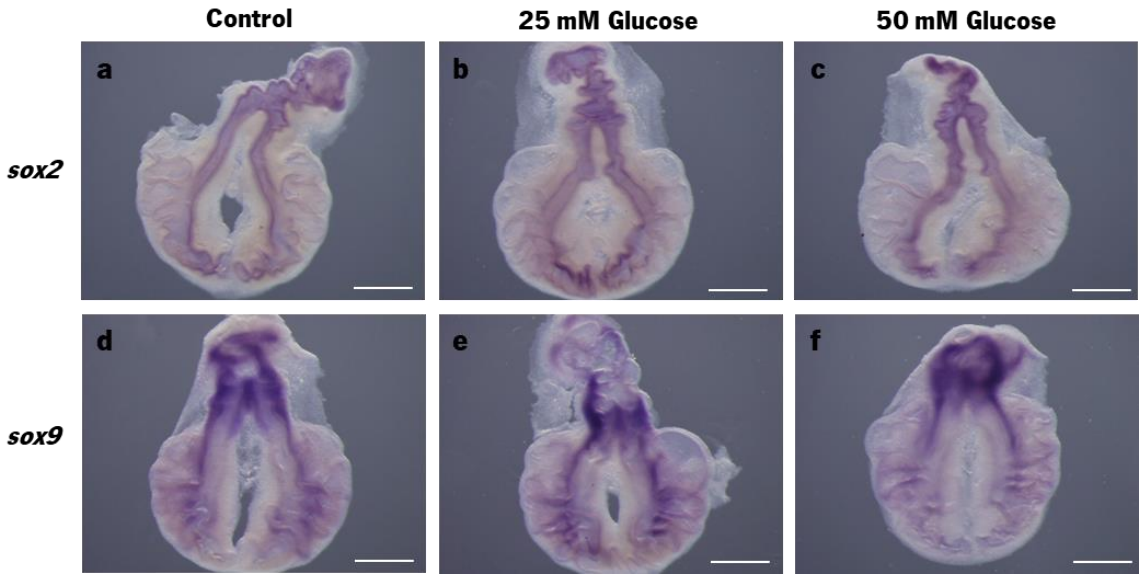

Figure 13 - *In vitro* chick lung explants supplemented with glucose, followed by *in situ* hybridization for *sox2* and *sox9*. Representative examples of D2 chick lung explants supplemented with 5.5 mM (control) (**a** and **d**), 25 mM (**b** and **e**) and 50 mM (**c** and **f**) of glucose, probed for *sox2* (**a**, **b**, **c**) and *sox9* (**d**, **e**, **f**). Scale bar: 500 µm. n ≥ 5 per condition.

Branching morphogenesis-related genes were evaluated by qPCR in lung explants supplemented with glucose and controls to understand if the signaling pathways involved in branching processes were altered. *fgf10* relative expression (**Fig. 14**a) showed a statistically significant decrease in lungs supplemented with 25 mM of glucose compared to controls (p=0.0127), and no differences were observed between 50 mM dose and controls. Furthermore, an increase in *fgf10* expression levels was detected in 50 mM dose compared to 25 mM-treated lungs (**Fig. 14**a; p=0.0041). Regarding *shh* expression (**Fig. 14**b), it is possible to observe a significant increase in the 50 mM dose compared to the 25 mM dose (p=0.0271). However, no differences were found between the controls and 25 mM and 50 mM doses. Lastly, a statistically significant decrease in *wnt7b* relative expression (**Fig. 14**c) was shown in 25 mM and 50 mM-treated lungs compared to the controls (p=0.0007; p=0.0013). Moreover, no differences were observed between 25 mM and 50 mM-treated lungs.

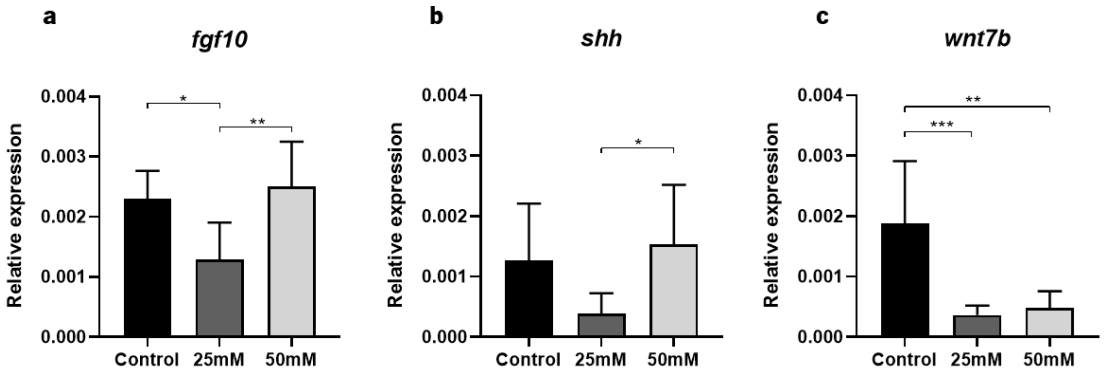

Figure 14 - mRNA expression levels of branching-related genes evaluated by qPCR. Relative expression of *fgf10* (**a**), *shh* (**b**) and *wnt7b* (**c**) in D2 chick lungs explants supplemented with 5.5 mM (control), 25 mM and 50 mM of glucose. Data on gene expression was normalized for the housekeeping actin-β. Results are represented as mean ± SD. Statistically significant results are presented as: * p<0.05, ** p<0.01 and *** p<0.001. n ≥ 6 per condition.

5. Discussion

Diabetes in pregnancy has been associated with severe consequences for the offspring. Whereas hyperglycemia exposure at later stages of development affects fetal organ maturation and, consequently, its normal function, exposure to high maternal glucose levels at early stages of embryonic development is known to affect organogenesis, leading to congenital malformations. Therefore, hyperglycemia is considered a major teratogenic factor associated with several congenital abnormalities, mainly in the cardiovascular and central nervous systems. However, there is a lack of information regarding the consequences of hyperglycemia on early lung development. In this sense, in this study, we aimed to unveil hyperglycemia-related alterations in branching morphogenesis and its underlying mechanisms. For this purpose, *in vitro* chick lung explants were exposed to increasing doses of glucose, supplemented in the culture medium, for 48 hours. In humans, normal fasting circulating glucose levels range from 4 to 5.4 mM, and hyperglycemia is defined by fasting plasma glucose levels above approximately 7 mM. On the other hand, normal blood glucose concentrations in the chicken range from approximately 12 to 30 mM. Thus, hyperglycemia in adult birds is described as glucose circulating levels above 30 mM (Datar and Bhonde, 2005). For this reason, the doses to induce hyperglycemia were 25, 50, or 75 mM.

After 48h, lung explants were morphometrically analyzed. The results showed that high glucose levels led to a decrease in the total area of the lung, as well as a decrease in the epithelial area and perimeter of the lung (**Fig. 6**), suggesting an impairment in early lung organogenesis. Moreover, branching was also decreased in lungs exposed to hyperglycemia, indicated by the reduced number of secondary buds formed after lung explant culture (**Fig. 6**). It has already been described that rat fetal lungs exposed to intrauterine maternal diabetes display a decrease in lung total tissue area at birth compared to controls (Koskinen *et al.*, 2012). Additionally, other morphological alterations have been found in mice embryonic lungs exposed to hyperglycemia using streptozotocin-induced mouse diabetic *in vivo* model, such as thickening of the alveolar walls, reduced alveolar air spaces, as well as decreased size and weight of embryonic mice lungs (He *et al.*, 2018). These alterations in lung morphology can impair lung development and maturation and consequently normal lung function, inducing severe post-natal consequences. In this sense, our results are in accordance with hyperglycemic-related alterations described at later stages of lung development, highlighting the importance of controlling maternal glucose levels to prevent hyperglycemia-induced lung consequences for the embryo.

The impact of hyperglycemia has already been reported in other early embryonic events. For instance, chicken embryos treated with high glucose levels exhibit a repression in somitogenesis together

with morphological alterations in the segmentation of the somites (Chen *et al.*, 2014). Furthermore, kidney malformations were also described in embryos of streptozotocin-induced diabetic female mice (Hokke *et al.*, 2013). In this study, an impairment in ureteric branching morphogenesis was observed, with a decrease in the number of ureteric tips and a deficit in nephrogenesis as a consequence of hyperglycemia in early embryonic development. The kidney and lung are organs that develop by branching morphogenesis and seem to display similar detrimental effects, reduction in the number of buds when exposed to a hyperglycemic environment pointing to a common response mechanism.

Glucose homeostasis depends on several signaling/hormonal systems that are simultaneously crucial for embryo development. For example, Insulin/IGF system, including insulin, IGF1 and IGF2, is important for normal embryo development, regulating fetal growth and development (Hiden *et al.*, 2009). Their action is mediated through their receptors and, particularly, it is known that IGF1 regulates lung development through its receptor IGF1R (Atar *et al.*, 2021). In fact, *igf1r* knockout mice display severe lung hypoplasia, leading to neonatal death due to respiratory distress (Epaud *et al.*, 2012). Furthermore, maternal diabetes and its consequences for the fetus have also been associated with insulin/IGF system impairment and deregulation of its components in maternal and fetal circulation (Hiden *et al.*, 2009). In this sense, we evaluated the expression pattern of *igf1r*, *igf2r* and *insr* in chick lung explants supplemented with high glucose levels, by *in situ* hybridization. First, the expression pattern of these receptors was characterized in the embryonic chick lung. *igf1r* is highly expressed in the epithelial compartment, mainly in the secondary bronchi and distal tips of the lung (**Fig. 7**), similarly to *igf1r* expression in the mammalian. In particular, in the embryonic mouse lung, *igf1r* is expressed in the epithelium rather than mesenchyme at later stages of development, although it seems that its expression can change throughout development (Kheirollahi *et al.*, 2022). *igf2r* is also present throughout the epithelium, although in lower levels compared to *igf1r* (**Fig. 8**). Likewise, *igf2r* appeared to be expressed in both mesenchyme and epithelium of branching sites in the embryonic mouse lung (Melnick *et al.*, 1996). Lastly, *insr* is faintly expressed in the epithelium of the secondary bronchi of the developing chick lung (**Fig. 9**). Although information regarding *insr* expression in the embryonic lung is lacking in the literature, *insr* was described to be expressed in fetal rat lung epithelial cells and a decrease in its expression was observed at later stages of lung development (Sodoyez-Goffaux *et al.*, 1981).

After hyperglycemia exposure, lung explants exhibited an increase in *igf1r* expression, especially in the two highest doses of glucose tested, compared to controls. Conversely, *igf2r* and *insr* expression appeared unaltered in glucose treated lung explants (**Fig. 10**). Some studies have already demonstrated the relation between increased expression of placental *igf1r* and *igf2r* in maternal diabetes, with diabetes-

related fetal health consequences (Ornoy *et al.*, 2021). Similarly, our results showed an increase in *igf1r* expression under hyperglycemic conditions on the embryonic lung. Thus, deregulation in the insulin/IGF system may be associated with impairment in embryo development, although the impact on early lung development has not been explored yet.

Considering the important role of metabolism in proper lung development, we further analyzed the expression of key glucose catabolism genes, to understand if any metabolic alterations could be associated with the lung organogenesis impairment observed in chick lung explants exposed to high glucose levels. The expression levels of *glut1* and *glut3,* responsible for the uptake of glucose from the extracellular area to the cytoplasm of the cells, were assessed by qPCR. The relative expression of these glucose transporters was decreased under hyperglycemic conditions, suggesting a reduction in the uptake of glucose by the lung tissue (**Fig. 11**). Similarly, studies using pre-implantation embryos with mouse models, also showed a decrease in GLUT1, GLUT2 and GLUT3 expression in the embryo, as a result of maternal hyperglycemia (Moley *et al.*, 1998). We hypothesize that the downregulation of glucose transporters, as a consequence of hyperglycemia, can be a mechanism to protect the embryo/lung from the increased glucose levels. However, it can lead to low glucose levels in the tissue, which can delay development, due to the decrease in the main energy source of the lung.

After glucose uptake by the cells, glucose is phosphorylated in glucose-6-phosphate in a reaction catalyzed by hexokinase (HK). Consequently, phosphofructokinase (PFK), a key glycolytic enzyme, will convert fructose-6-phosphate and ATP, into fructose-1,6-biphosphate and ADP, respectively. In hyperglycemic conditions, a decrease in the expression levels of *hk1* and *pfk1* key glycolytic enzymes was observed, indicating once again a decrease in glucose catabolism in the embryonic lung (**Fig. 11**). The decreased expression of *hk1* and *pfk1* can be associated with the possible decrease in glucose transport, as a consequence of reduced expression of *gluts*. Nevertheless, considering the enhanced metabolic needs of the embryonic lung tissue at this stage of development, the decrease of these two glycolytic enzymes would not be expected. However, a decrease in the glycolytic metabolism and, consequently, in the production of energy by the tissue may justify the impairment in lung development observed under hyperglycemic conditions.

At the end of glycolysis, one molecule of glucose will be converted into two molecules of pyruvate, which can then be converted into lactate by the enzyme lactate dehydrogenase (LDH); or it can be converted into acetyl-Coa by pyruvate dehydrogenase (PDH), and then incorporated in the TCA cycle in the mitochondria. In this work, *ldhb* expression appeared to be increased in lung explants supplemented with high glucose levels, especially in branching regions, while *ldha* expression remained unaltered (**Fig.**

12). The expression pattern of both LDHs in the embryonic chick lung is in agreement with what has already been described in previous studies (Fernandes-Silva *et al.*, 2021). These results suggest an increase in lactate conversion into pyruvate, due to the increase in *ldhb* expression. Pyruvate can then enter the TCA cycle in the mitochondria to produce energy, which may compensate for the downregulation of glycolysis, as a consequence of diminished *gluts*, *hk1* and *pfk1* expression levels. Overall, our results showed that the metabolic component of the chick embryo lung is altered in hyperglycemia-exposed lungs (**Fig. 15**).

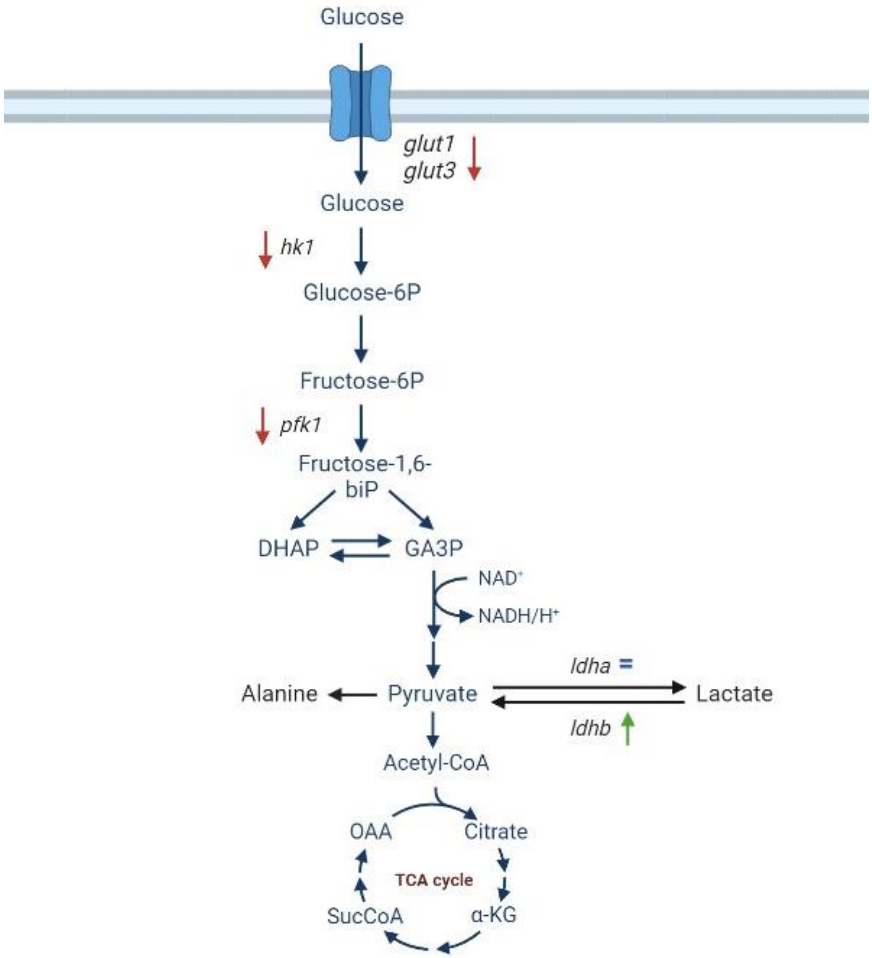

Figure 15 – Representation of the impact of hyperglycemia in glucose metabolism of the chick embryonic lung. Arrows represent a decrease (red) or an increase (green) in the expression of the respective transcripts. The symbol (=) represents that the transcript maintains its expression levels.

LDHs expression pattern has been recently associated with active proliferation sites in the embryonic chick lung (Fernandes-Silva *et al.*, 2021); conversely, our results show increased *ldhb* expression, but a decrease in lung branching morphogenesis. Thus, other pathways may be involved in the decrease in lung branching after hyperglycemia exposure, such as key players involved in lung patterning and branching processes.

In this context, we assessed the expression of lung patterning and branching-related genes, to elucidate the mechanisms triggering the hyperglycemic-related alterations observed in chick lung development. Regarding lung patterning related genes, the expression of *sox2* and *sox9*, responsible for the differentiation of proximal and distal respiratory airways, respectively, was evaluated. *sox2* and *sox9* expression pattern is in accordance with previous studies using the chicken embryo lung (Fernandes-Silva, Vaz-Cunha, et al., 2017). No differences were observed in the expression pattern of *sox2* between the experimental groups; however, *sox9* expression seems to decrease in the most distal region of lungs treated with the highest dose of glucose, which might point to an impairment of the distal lung progenitor's fate (**Fig. 13**).

Furthermore, the expression of branching molecular players, namely FGF10, SHH and WNT7b was evaluated in lung explants exposed to hyperglycemia by qPCR (**Fig. 14**). We observed a decrease in *fgf10* and *wnt7b* expression levels in 25 mM-treated lungs when compared to controls; regarding *shh* expression levels, no differences were detected. However, these molecular alterations did not impact lung morphology or branching. Conversely, in 50 mM-treated lungs, *fgf10* and *shh* expression levels remained unaltered and *wnt7b* expression was significantly decreased; in this case, we observed impaired lung growth and branching. Considering the 50 mM phenotype, one could expect to find an impairment in *fgf10* and *shh* expression levels given their role in regulating branching morphogenesis. Decreased *wnt7b* expression detected in glucose-treated lungs may be associated with the reduction in lung branching and growth observed in the highest dose of glucose tested. In fact, *wnt7b* knockout mice exhibit hypoplastic lungs (Shu *et al.*, 2002). Nevertheless, different studies have shown that *shh* knockout mice did not alter *wnt7b* expression in the embryonic lungs (Pepicelli *et al.*, 1998) and also that FGF signaling is not essential for WNT activity in mice embryonic lungs (Shu *et al.*, 2005). Thus, due to the complexity of the molecular network involved in early lung development, it is likely that other molecular players besides *wnt7b* may contribute to the hyperglycemic-related lung phenotype.

Recent studies have shown that hyperglycemia exposure *in ovo*, using the chicken embryo model, has been associated with congenital heart and limb defects, which has been linked to a reduction in *shh* signaling pathway (Ding *et al.*, 2020). Nevertheless, in our study, high glucose levels did not affect *shh* expression in the embryonic chick lung. SHH signaling is a key developmental pathway that may have a different behavior depending on the organ and stage of development. Moreover, a downregulation of WNT signaling, as well as its intermediates, such as FZD and β-catenin, has been described in the cardiac outflow tract (OFT) in embryonic mice exposed to maternal hyperglycemia, being associated with severe abnormalities in the OFT (Zhao, 2014). Furthermore, impaired kidney development induced by a murine

maternal diabetes model, has been associated with an upregulation of HHIP, a downstream target of SHH signaling (Zhao *et al.*, 2014). Therefore, hyperglycemia can impair several signaling pathways, which have distinct adverse effects on different organs, thus compromising normal organogenesis.

Altogether, the results showed that hyperglycemia impacts early chick lung organogenesis at the morphological, metabolic, and molecular levels. The alterations observed can contribute to congenital lung malformations and other respiratory outcomes, which can compromise post-natal respiratory health.

6. Final Remarks and Future Perspectives

The teratogenic effect of hyperglycemia is well known and different consequences for the offspring have already been described. Nevertheless, the impact of hyperglycemia on embryonic lung development remains poorly understood. In this sense, our study uncovered that, in fact, hyperglycemia exposure at early stages of lung organogenesis impairs lung growth and development. Moreover, metabolic and molecular alterations were observed associated with high glucose levels exposure in the chick lung.

Regarding lung growth, we observed a reduction in lung size when explants were exposed to the highest dose of glucose. Likewise, a decrease in lung branching was also detected, with a reduction in the secondary buds formed after lung explant culture. Thus, hyperglycemia induced morphological alterations in the chick embryonic lung, leading to an impairment in lung growth and branching.

Afterwards, we elucidated the mechanisms that could be eliciting these morphological alterations in the embryonic chick lung. Indeed, the expression levels of glucose transporters *glut1* and *glut3* were diminished, as well as glycolytic enzymes *hk1* and *pfk1*. These results suggest that hyperglycemia reprograms lung metabolism and induces a decrease in glucose uptake by the tissue, and, consequently, a downregulation in the glycolytic metabolism. In this regard, a metabolomics analysis could be performed to analyze the presence of different metabolites in the culture medium and confirm whether the molecular data reflects a decrease in the uptake of glucose and corroborate our findings.

Moreover, *ldhb* expression increases after hyperglycemia exposure, suggesting that there is an enhanced interconversion of lactate into pyruvate, which can undergo into the TCA cycle. Considering that the glycolytic pathway might be decreased, the tissue may perhaps compensate the lack of energy production in its most effective way and increase oxidative phosphorylation (OXPHOS) to obtain energy. However, taking into account the high proliferative rates and the metabolic requirements at this stage of development, the energy obtained by OXPHOS could not be adequate to sustain the developing tissue needs. This might explain the impairment in lung growth observed in hyperglycemic-exposed lungs. In this sense, a seahorse assay could be performed to evaluate oxygen consumption in the tissue and determine if there is indeed an increase in OXPHOS in the mitochondria. For this purpose, OXPHOS-related proteins, such as the mitochondrial complexes involved in electron transfer, could also be analyzed by Western Blot.

Lung patterning-related genes, such as *sox2* and *sox9*, were also evaluated after hyperglycemia exposure. While *sox2* expression pattern appears to be unaltered, *sox9* seems to decrease its expression levels in the most distal region of the lung, under hyperglycemic conditions. However, quantitative

methods could be performed in the future, for instance, qPCR or western blot, to confirm these results, since *in situ* hybridization is a semi-quantitative method.

FGF10, SHH and WNT7B signaling members were also evaluated to understand the mechanisms underlying the hyperglycemic-related alterations observed in lung branching and growth. It is well established that lung organogenesis is an extremely complex process that is finely regulated by several signaling pathways. The interplay between these pathways is so intricate that it is virtually impossible to explain an abnormal lung phenotype considering only FGF, SHH and WNT. In this particular case, other molecular players might be involved in the morphological and branching alterations observed. In this sense, other signaling pathways should be evaluated in the future, as for instance Hippo signaling, that may trigger the hyperglycemic-associated lung defects.

In conclusion, hyperglycemia can affect early lung development and further studies are needed to uncover the molecular mechanisms underlying hyperglycemia related adverse effects on early lung development.

7. References

Alwan, S., and Chambers, C. (2015). Identifying Human Teratogens: An Update. *Journal of Pediatric Genetics*, *4*(2), 39–041.

Aros, C. J., Pantoja, C. J., and Gomperts, B. N. (2021). Wnt signaling in lung development, regeneration, and disease progression. *Communications Biology*, *4*(1), 1–13.

Atar, H. Y., Baatz, J. E., and Ryan, R. M. (2021). Molecular Mechanisms of Maternal Diabetes Effects on Fetal and Neonatal Surfactant. *Children*, *8*(4), 1–10.

Azad, M. B., Moyce, B. L., Guillemette, L., Pascoe, C. D., Wicklow, B., McGavock, J. M., Halayko, A. J., and Dolinsky, V. W. (2017). Diabetes in pregnancy and lung health in offspring: developmental origins of respiratory disease. *Paediatric Respiratory Reviews*, *21*(1), 19–26.

Baack, M. L., Forred, B. J., Larsen, T. D., Jensen, D. N., Wachal, A. L., Khan, M. A., and Vitiello, P. F. (2016). Consequences of a maternal high-fat diet and late gestation diabetes on the developing rat lung. *PLoS ONE*, *11*(8), 1–21.

Bednarczyk, M., Dunislawska, A., Stadnicka, K., and Grochowska, E. (2021). Chicken embryo as a model in epigenetic research. *Poultry Science*, *100*(7), 1–12.

Bianco, M. E., and Josefson, J. L. (2019). Hyperglycemia During Pregnancy and Long-Term Offspring Outcomes. *Current Diabetes Reports*, *19*(12), 1–14.

Biga, L. M., Dawson, S., Harwell, A., Hopkins, R., Kaufmann, J., Lemaster, M., Matern, P., Morrison-Graham, K., Quick, D., and Runyeon, J. (2008). Development and Inheritance. In *Anatomy* and *Physiology* (Vol. 28, Issue 1, pp. 5–7).

Bjørnstad, S., Austdal, L. P. E., Roald, B., Glover, J. C., and Paulsen, R. E. (2015). Cracking the egg: Potential of the developing chicken as a model system for nonclinical safety studies of pharmaceuticals. *Journal of Pharmacology and Experimental Therapeutics*, *355*(3), 386–396.

Boukouris, A. E., Zervopoulos, S. D., and Michelakis, E. D. (2016). Metabolic Enzymes Moonlighting in the Nucleus: Metabolic Regulation of Gene Transcription. *Trends in Biochemical Sciences*, *41*(8), 712–730.

Bulusu, V., Prior, N., Snaebjornsson, M. T., Kuehne, A., Sonnen, K. F., Kress, J., Stein, F., Schultz, C., Sauer, U., and Aulehla, A. (2017). Spatiotemporal Analysis of a Glycolytic Activity Gradient Linked to Mouse Embryo Mesoderm Development. *Developmental Cell*, *40*(4), 331–341.

Cai, L., Sutter, B. M., Li, B., and Tu, B. P. (2011). Acetyl-CoA Induces Cell Growth and Proliferation by Promoting the Acetylation of Histones at Growth Genes. *Molecular Cell*, *42*(4), 426–437.

Caldeira, I., Fernandes-Silva, H., Machado-Costa, D., Correia-Pinto, J., and Moura, R. S. (2021). Developmental pathways underlying lung development and congenital lung disorders. *Cells*, *10*(11), 1–27.

Chen, Y., Wang, G., Ma, Z. lai, Li, Y., Wang, X. yu, Cheng, X., Chuai, M., Tang, S. ze, Lee, K. K. H., and Yang, X. (2014). Adverse effects of high glucose levels on somite and limb development in avian embryos. *Food and Chemical Toxicology*, *71*(1), 1–9.

Craig, M. E., Hattersley, A., and Donaghue, K. C. (2009). Definition, epidemiology and classification of diabetes in children and adolescents. *Pediatric Diabetes*, *10*(12), 3–12.

Dady, A., Blavet, C., and Duband, J. L. (2012). Timing and kinetics of E- to N-cadherin switch during neurulation in the avian embryo. *Developmental Dynamics*, *241*(8), 1333–1349.

Datar, S., and Bhonde, R. R. (2005). Shell-Less Chick Embryo Culture as an Alternative in vitro Model to Investigate Glucose-Induced Malformations in Mammalian Embryos. *The Review of Diabetic Studies*, *2*(4), 221–221.

DiMeglio, L. A., Evans-Molina, C., and Oram, R. A. (2019). Type 1 Diabetes. *Lancet*, *176*(3), 139–148.

Ding, Z., Zhou, H., McCauly, N., Ko, G., Zhang, K. K., and Xie, L. (2020). In ovo hyperglycemia causes congenital limb defects in chicken embryos via disruption of cell proliferation and apoptosis. *Biochimica et Biophysica Acta - Molecular Basis of Disease*, *1866*(12), 1–10.

Dohle, D. S., Pasa, S. D., Gustmann, S., Laub, M., Wissler, J. H., Jennissen, H. P., and Dünker, N. (2010). Chick ex ovo culture and ex ovo CAM assay: How it really works. *Journal of Visualized Experiments*, *33*(1), 1–6.

Domowicz, M. S., Henry, J. G., Wadlington, N., Navarro, A., Kraig, R. P., and Schwartz, N. B. (2011). Astrocyte precursor response to embryonic brain injury. *Brain Research*, *1389*(1), 35–49.

el Azhar, Y., and Sonnen, K. F. (2021). Development in a Dish—In Vitro Models of Mammalian Embryonic Development. *Frontiers in Cell and Developmental Biology*, *9*(655993), 1–8.

Epaud, R., Aubey, F., Xu, J., Chaker, Z., Clemessy, M., Dautin, A., Ahamed, K., Bonora, M., Hoyeau, N., Fléjou, J. F., Mailleux, A., Clement, A., Henrion-Caude, A., and Holzenberger, M. (2012). Knockout of insulin-like growth factor-1 receptor impairs distal lung morphogenesis. *PloS One*, *7*(11), 1–12.

Fernandes-Silva, H., Alves, M. G., Araújo-Silva, H., Silva, A. M., Correia-Pinto, J., Oliveira, P. F., and Moura, R. S. (2021). Lung branching morphogenesis is accompanied by temporal metabolic changes towards a glycolytic preference. *Cell and Bioscience*, *11*(1), 1–18.

Fernandes-Silva, H., Correia-Pinto, J., and Moura, R. S. (2017). Canonical sonic hedgehog signaling in early lung development. *Journal of Developmental Biology*, *5*(3), 1–14.

Fernandes-Silva, H., Vaz-Cunha, P., Barbosa, V. B., Silva-Gonçalves, C., Correia-Pinto, J., and Moura, R. S. (2017). Retinoic acid regulates avian lung branching through a molecular network. *Cellular and Molecular Life Sciences*, *74*(24), 4599–4619.

Gándara, L., and Wappner, P. (2018). Metabo-Devo: A metabolic perspective of development. *Mechanisms of Development*, *154*(1), 12–23.

Guariguata, L., Linnenkamp, U., Beagley, J., Whiting, D. R., and Cho, N. H. (2014). Global estimates of the prevalence of hyperglycaemia in pregnancy. *Diabetes Research and Clinical Practice*, *103*(2), 176–185.

Hamburger, V., and Hamilton, H. L. (1951). A series of normal stages in the development of the chick embryo. *Journal of Morphology*, *88*(1), 49–92.

He, M., Wang, G., Han, S., Li, K., Jin, Y., Liu, M., Si, Z., Wang, J., Liu, G., and Yang, X. (2018). Negative impact of hyperglycaemia on mouse alveolar development. *Cell Cycle*, *17*(1), 80–91.

Hiden, U., Glitzner, E., Hartmann, M., and Desoye, G. (2009). Insulin and the IGF system in the human placenta of normal and diabetic pregnancies. *Journal of Anatomy*, *215*(1), 60–68.

Hokke, S. N., Armitage, J. A., Puelles, V. G., Short, K. M., Jones, L., Smyth, I. M., Bertram, J. F., and Cullen-McEwen, L. A. (2013). Altered Ureteric Branching Morphogenesis and Nephron Endowment in Offspring of Diabetic and Insulin-Treated Pregnancy. *PLoS ONE*, *8*(3), 1–9.

Hu, D., Young, N. M., Li, X., Xu, Y., Hallgrımsson, B., and Marcucio, R. S. (2015). A dynamic shh expression pattern, regulated by shh and bmp signaling, coordinates fusion of primordia in the amniote face. *Development*, *142*(3), 567–574.

IDF. (2021). IDF Diabetes Atlas 2021. In *International Diabetes Federation*. https://doi.org/10.1016/j.diabres.2013.10.013

Kheirollahi, V., Khadim, A., Kiliaris, G., Korfei, M., Barroso, M. M., Alexopoulos, I., Vazquez-Armendariz, A. I., Wygrecka, M., Ruppert, C., Guenther, A., Seeger, W., Herold, S., and El Agha, E. (2022). Transcriptional Profiling of Insulin-like Growth Factor Signaling Components in Embryonic Lung Development and Idiopathic Pulmonary Fibrosis. *Cells*, *11*(1973), 1–14.

Korn, M. J., and Cramer, K. S. (2007). Windowing chicken eggs for developmental studies. *Journal of Visualized Experiments*, *8*(1), 1–2.

Koskinen, A., Lukkarinen, H., Moritz, N., Aho, H., Kääpä, P., and Soukka, H. (2012). Fetal hyperglycemia alters lung structural development in neonatal rat. *Pediatric Pulmonology*, *47*(3), 275–282.

Liu, G., and Summer, R. (2019). Cellular Metabolism in Lung Health and Disease. *Physiology* and *Behavior*, *10*(81), 403–428.

Livak, K. J., and Schmittgen, T. D. (2001). Analysis of relative gene expression data using real-time quantitative PCR and the 2-ΔΔCT method. *Methods*, *25*(4), 402–408.

Maina, J. N. (2003). A systematic study of the development of the airway (bronchial) system of the avian lung from days 3 to 26 of embryogenesis: A transmission electron microscopic study on the domestic fowl, Gallus gallus variant domesticus. *Tissue and Cell*, *35*(5), 375–391.

Maina, J. N. (2012). Comparative molecular developmental aspects of the mammalian- and the avian lungs, and the insectan tracheal system by branching morphogenesis: recent advances and future directions. *Frontiers in Zoology*, *9*(16), 1–31.

Melnick, M., Chen, H., Rich, K. A., and Jaskoll, T. (1996). Developmental expression of insulin-like growth factor II receptor (IGF-IIR) in congenic mouse embryonic lungs: Correlation between IGF-IIR mRNA and protein levels and heterochronic lung development. *Molecular Reproduction and Development*, *44*(2), 159–170.

Miyazawa, H., and Aulehla, A. (2018). Revisiting the role of metabolism during development. *Development (Cambridge)*, *145*(19), 1–11.

Moley, K. H., Chi, M. M. Y., and Mueckler, M. M. (1998). Maternal hyperglycemia alters glucose transport and utilization in mouse preimplantation embryos. *American Journal of Physiology - Endocrinology and Metabolism*, *275*(1), 38–47.

Moura, R. S. (2019). Retinoic Acid as a Modulator of Proximal-Distal Patterning and Branching Morphogenesis of the Avian Lung. In *Methods in Molecular Biology* (Vol. 2019, pp. 209–224).

Moura, R. S., Carvalho-Correia, E., DaMota, P., and Correia-Pinto, J. (2014). Canonical Wnt signaling activity in early stages of chick lung development. *PLoS ONE*, *9*(12), 1–27.

Moura, R. S., and Correia-Pinto, J. (2017). Molecular Aspects of Avian Lung Development. In *The Biology of the Avian Respiratory System* (pp. 129–146).

Moura, R. S., Coutinho-Borges, J. P., Pacheco, A. P., DaMota, P. O., and Correia-Pinto, J. (2011). FGF signaling pathway in the developing chick lung: Expression and inhibition studies. *PLoS ONE*, *6*(3), 1–10.

Moura, R. S., Silva-Gonçalves, C., Vaz-Cunha, P., and Correia-Pinto, J. (2016). Expression analysis of Shh signaling members in early stages of chick lung development. *Histochemistry and Cell Biology*, *146*(4), 457–466.

Oginuma, M., Moncuquet, P., Xiong, F., Karoly, E., Chal, J., Guevorkian, K., and Pourquié, O. (2017). A gradient of glycolytic activity coordinates FGF and Wnt signaling during elongation of the body axis in amniote embryos. *Developmental Cell*, *40*(4), 342–353.

Ogurtsova, K., Guariguata, L., Barengo, N. C., Ruiz, P. L. D., Sacre, J. W., Karuranga, S., Sun, H., Boyko, E. J., and Magliano, D. J. (2022). IDF diabetes Atlas: Global estimates of undiagnosed diabetes in adults for 2021. *Diabetes Research and Clinical Practice*, *183*(109118), 1–8.

Ornoy, A., Becker, M., Weinstein-Fudim, L., and Ergaz, Z. (2021). Diabetes during pregnancy: A maternal disease complicating the course of pregnancy with long-term deleterious effects on the offspring. a clinical review. *International Journal of Molecular Sciences*, *22*(6), 1–38.

Pepicelli, C. V., Lewis, P. M., and McMahon, A. P. (1998). Sonic hedgehog regulates branching morphogenesis in the mammalian lung. *Current Biology*, *8*(19), 1083–1086.

Petersmann, A., Müller-Wieland, D., Müller, U. A., Landgraf, R., Nauck, M., Freckmann, G., Heinemann, L., and Schleicher, E. (2019). Definition, Classification and Diagnosis of Diabetes Mellitus. *Experimental and Clinical Endocrinology and Diabetes*, *127*(1), 1–7.

Punthakee, Z., Goldenberg, R., and Katz, P. (2018). Definition, Classification and Diagnosis of Diabetes, Prediabetes and Metabolic Syndrome. *Canadian Journal of Diabetes*, *42*(1), 10–15.

Rahman, M. S., Hossain, K. S., Das, S., Kundu, S., Adegoke, E. O., Rahman, M. A., Hannan, M. A., Uddin, M. J., and Pang, M. G. (2021). Role of insulin in health and disease: An update. *International Journal of Molecular Sciences*, *22*(12), 1–19.

Rashidi, H., and Sottile, V. (2009). The chick embryo: Hatching a model for contemporary biomedical research. *BioEssays*, *31*(4), 459–465.

Rossant, J., and Tam, P. P. L. (2022). Early human embryonic development: Blastocyst formation to gastrulation. *Developmental Cell*, *57*(2), 152–165.

Sakiyama, J. I., Yamagishi, A., and Kuroiwa, A. (2003). Tbx4-Fgf10 system controls lung bud formation during chicken embryonic development. *Development*, *130*(7), 1225–1234.

Sekine, K., Ohuchi, H., Fujiwara, M., Yamasaki, M., Yoshizawa, T., Sato, T., Yagishita, N., Matsui, D., Koga, Y., Itoh, N., and Kato, S. (1999). Fgf10 is essential for limb and lung formation. *Nature Genetics*, *21*(1), 138–141.

Shi, L., Ko, M. L., Huang, C. C. Y., Park, S. Y., Hong, M. P., Wu, C., and Ko, G. Y. P. (2014). Chicken Embryos as a Potential New Model for Early Onset Type i Diabetes. *Journal of Diabetes Research*, *2014*(1), 1–10.

Shu, W., Guttentag, S., Wang, Z., Andl, T., Ballard, P., Lu, M. M., Piccolo, S., Birchmeier, W., Whitsett, J. A., Millar, S. E., and Morrisey, E. E. (2005). Wnt/β-catenin signaling acts upstream of N-myc, BMP4, and FGF signaling to regulate proximal-distal patterning in the lung. *Developmental Biology*, *283*(1), 226–239.

Shu, W., Jiang, Y. Q., Lu, M. M., and Morrisey, E. E. (2002). Wnt7b regulates mesenchymal proliferation and vascular development in the lung. *Development*, *129*(20), 4831–4842.

Sodoyez-Goffaux, F. R., Sodoyez, J. C., and Vos, C. J. De. (1981). Insulin Receptors in the Fetal Rat Lung. A Transient Characteristic of Fetal Cells? *Pediatric Research*, *15*(1), 1303–1307.

Stern, C. D. (2004). The chick embryo - Past, present and future as a model system in developmental biology. *Mechanisms of Development*, *121*(9), 1011–1013.

Sun, H., Saeedi, P., Karuranga, S., Pinkepank, M., Ogurtsova, K., Duncan, B. B., Stein, C., Basit, A., Chan, J. C. N., Mbanya, J. C., Pavkov, M. E., Ramachandaran, A., Wild, S. H., James, S., Herman, W. H., Zhang, P., Bommer, C., Kuo, S., Boyko, E. J., and Magliano, D. J. (2022). IDF Diabetes Atlas: Global, regional and country-level diabetes prevalence estimates for 2021 and projections for 2045. *Diabetes Research and Clinical Practice*, *183*(109119), 1–13.

Sweeting, A. N., Ross, G. P., Hyett, J., Molyneaux, L., Constantino, M., Harding, A. J., and Wong, J. (2016). Gestational Diabetes Mellitus in Early Pregnancy: Evidence for Poor Pregnancy Outcomes Despite Treatment. *Diabetes Care*, *39*(1), 75–81.

Tan, S. Y., Mei Wong, J. L., Sim, Y. J., Wong, S. S., Mohamed Elhassan, S. A., Tan, S. H., Ling Lim, G. P., Rong Tay, N. W., Annan, N. C., Bhattamisra, S. K., and Candasamy, M. (2019). Type 1 and 2 diabetes mellitus: A review on current treatment approach and gene therapy as potential intervention. *Diabetes and Metabolic Syndrome: Clinical Research and Reviews*, *13*(1), 364–372.

Weiss, U., Cervar, M., Puerstner, P., Schmut, O., Haas, J., Mauschitz, R., Arikan, G., and Desoye, G. (2001). Hyperglycaemia in vitro alters the proliferation and mitochondrial activity of the choriocarcinoma cell lines BeWo , JAR and JEG-3 as models for human first-trimester trophoblast. *Diabetologia*, *44*(1), 209–219.

WHO. (2014). Diagnostic criteria and classification of hyperglycaemia first detected in pregnancy: a World Health Organization Guideline. *Diabetes Research and Clinical Practice*, *103*(3), 341–363.

WHO. (2016). *Global Report on Diabetes*. *978*, 1–86.

Wolpert, L. (2004). Much more from the chicken's egg than breakfast - A wonderful model system. *Mechanisms of Development*, *121*(9), 1015–1017.

Yammine, S., and Latzin, P. (2020). Normal Lung Development in Relation to Clinical Practice and the Impact of Environment on Development. In *Encyclopedia of Respiratory Medicine* (Issue 2, pp. 1–14).

Young, J. J., Grayson, P., Edwards, S. V., and Tabin, C. J. (2019). Attenuated Fgf signaling underlies the forelimb heterochrony in the emu Dromaius novaehollandiae. *Current Biology*, *29*(21), 3681–3691.

Zhao, X. P., Liao, M. C., Chang, S. Y., Abdo, S., Aliou, Y., Chenier, I., Ingelfinger, J. R., and Zhang, S. L. (2014). Maternal diabetes modulates kidney formation in murine progeny: The role of hedgehog interacting protein (HHIP). *Diabetologia*, *57*(9), 1986–1996.

Zhao, Z. (2014). TGFβ and Wnt in cardiac outflow tract defects in offspring of diabetic pregnancies. *Birth Defects Research. Part B, Developmental and Reproductive Toxicology*, *101*(5), 364–370.

Zheng, Y., Ley, S. H., and Hu, F. B. (2018). Global aetiology and epidemiology of type 2 diabetes mellitus and its complications. *Nature Reviews Endocrinology*, *14*(2), 88–98.

Zhu, Y., Li, Y., Wei, J., and Liu, X. (2012). The role of sox genes in lung morphogenesis and cancer. *International Journal of Molecular Sciences*, *13*(12), 15767–15783.

8. Appendix I

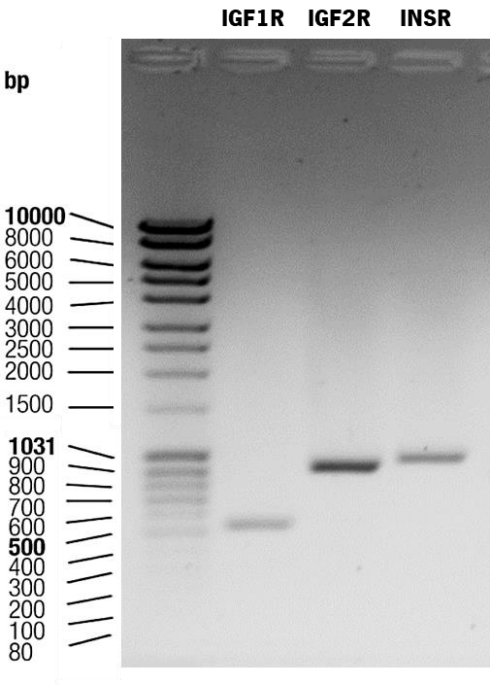

Supplementary Figure 1 – Primer testing for *igf1r*, *igf2r* and *insr*. Primers were tested using cDNA from a HH25 embryo as a template in conventional PCR, followed by an agarose gel 1%. Fragments were then cloned into the pCR™II-TOPO® vector. The first lane of the gel corresponds to DNA molecular weight ladder (MassRuler DNA Ladder Mix, ThermoFisher).

Supplementary Figure 2 – *igf1r*, *igf2r* and *insr* expression pattern in the chicken embryo. Representative example of whole mount *in situ* hybridization of HH25 embryos. Scale bar: 1 mm.